

Article

The Biodiversity of Calcaxonian Octocorals from the Irish Continental Slope Inferred from Multilocus Mitochondrial Barcoding

Declan Morrissey^{1,*}, Candice B. Untiedt², Karen Croke¹, Aisling Robinson¹, Eva Turley¹ and A. Louise Allcock¹

¹ School of Natural Sciences and Ryan Institute, National University of Ireland Galway, H91 TK33 Galway, Ireland; karencroke91@gmail.com (K.C.); a.robinson6@nuigalway.ie (A.R.); e.turley@hotmail.com (E.T.); louise.allcock@nuigalway.ie (A.L.A.)

² CSIRO Oceans and Atmosphere and School of Natural Sciences Hobart, University of Tasmania, Hobart, TAS 7005, Australia; candice.untiedt@csiro.au

* Correspondence: d.morrissey4@nuigalway.ie or declanmorrissey4@gmail.com

Abstract: Deep-sea corals are important benthic inhabitants that support the biodiversity and function of the wider faunal community; however, their taxonomy is underdeveloped and their accurate identification is often difficult. In our study, we investigated the utility of a superextended (>3000 bp) barcode and explored the effectiveness of various molecular species delimitation techniques with an aim to put upper and lower bounds on the estimated number of calcaxonian species in Irish waters. We collected 112 calcaxonians (70 Keratoisididae, 22 Primnoidae, 20 Chrysogorgiidae) and one chelidonisid from the Irish continental slope and sequenced a 3390 bp DNA barcode comprising four mitochondrial regions (*mtMutS*, *COI* + *igr1*, 16S rRNA-*ND2*, and *igr4*), recovering 38 haplotypes. Individuals that shared a haplotype were often morphologically distinct, and we thus undertook detailed morphological work, including SEM of sclerites, on one representative of each morphotype within each haplotype. GMYC, bGMYC, and mPTP returned incongruent estimates of species numbers. In total, there are between 25 and 40 species, although no definitive number could be assigned, primarily due to poorly defined keratoisidid species boundaries. As expected, the superextended barcode provided greater discrimination power than single markers; bGMYC appeared to be the most effective delimiter. Among the identified species were *Chelidonisis aurantiaca*, collected deeper than previously known at 1507 m, and *Calyptrophora clinata*, recorded for the second time from the Northeast Atlantic. A full understanding of the diversity and distribution of calcaxonians requires substantial taxonomic work, but we highlight the Irish continental slope as harbouring significant diversity.

Keywords: Keratoisididae; Primnoidae; Chrysogorgiidae; Chelidonisididae; deep sea; species delimitation; Irish Margin; bathyal diversity; octocorals; DNA barcoding



Citation: Morrissey, D.; Untiedt, C.B.; Croke, K.; Robinson, A.; Turley, E.; Allcock, A.L. The Biodiversity of Calcaxonian Octocorals from the Irish Continental Slope Inferred from Multilocus Mitochondrial Barcoding. *Diversity* **2022**, *14*, 576. <https://doi.org/10.3390/d14070576>

Academic Editors: Michael Wink, Saskia Brix and James Taylor

Received: 29 May 2022

Accepted: 14 July 2022

Published: 18 July 2022

Publisher's Note: MDPI stays neutral with regard to jurisdictional claims in published maps and institutional affiliations.



Copyright: © 2022 by the authors. Licensee MDPI, Basel, Switzerland. This article is an open access article distributed under the terms and conditions of the Creative Commons Attribution (CC BY) license (<https://creativecommons.org/licenses/by/4.0/>).

1. Introduction

The deep sea is the largest and least-explored ecosystem on the planet [1]. Geomorphic features found on continental slopes have been discovered to harbour increased biodiversity; for example, submarine canyons [2], seamounts [3], and cold-water coral reefs [4]. Situated in the Northeast Atlantic at the northwestern edge of Europe, Ireland has a marine territory of ~880,000 km², ten times that of its landmass, which encompasses an extensive continental slope heavily incised with canyons and gullies across its entirety. These complex topographies at the shelf edge and slope interact with the overlying water, affecting local oceanographic and hydrodynamic conditions which promote biodiversity [5]. Such enhanced biodiversity is evident; for example, in Ireland's carbonate mound provinces where residual bottom currents are increased [6]; in the Whittard Canyon system where a

unique biotope comprising the large bivalves *Acesta excavata* (Fabricius, 1779) and *Neopycnodonte zibrowii* Gofas, Salas and Taviani, 2009 is found at 600–800 m where internal waves resuspend particulate matter [7]; and through species distribution modelling that predicts increased species richness and a greater likelihood of corals in areas of Whittard Canyon with elevated currents and complex topography [8].

Octocorals are important benthic constituents in the deep sea, capable of forming dense aggregations referred to as coral gardens. These gardens are important for the wider faunal community. They provide a significant structural role, as octocorals house unique commensal species on their branches [9], harbour eggs of charismatic species such as catsharks [10] and cephalopods [11], and act as a nursery for juvenile invertebrates, e.g., basket stars [12]. Many corals are slow-growing and long-lived, with radiocarbon (^{14}C) ageing of some individuals of *Paramuricea* sp. and *Chrysogorgia* sp. showing 464 years and 192 years, respectively, with the upper estimates of *Paramuricea* exceeding 600 years [13]. These life-history traits, combined with the important ecosystem functions provided by deep-sea corals, have led to concern over the potential effect of fishing impacts on these ecosystems, which have been designated as Vulnerable Marine Ecosystems (VMEs) and now require States to implement appropriate conservation measures to protect them through standard reporting and monitoring.

Certain groups of octocorals are prevalent in the deep sea; for example, within the sub-order Calcaxonia (Order Alcyonacea), there are three widely distributed families: Chrysogorgiidae, Keratoisididae, and Primnoidae [9]. A lack of knowledge on definitive species boundaries, scarcity of information regarding intraspecific variation and what morphological characters are taxonomically important, and deficiencies in species descriptions in the older literature are the root cause of the difficulty identifying octocorals' species, which is further exacerbated by the lack of taxonomic expertise. This is evident in the Keratoisididae, where there is widespread polyphyly at the genus rank due to the historic diagnosis of genera using branching pattern [14,15]. *Isidella* was diagnosed by nodal branching in a single plane, *Acanella* by nodal branching in multiple planes, *Keratoisis* by internodal branching, and *Lepidisis* by lack of branching. Branching pattern is now known to be labile [14,15], and species formerly thought to be congeneric are now known not to be. Recent taxonomic work has been undertaken to untangle the observed polyphyly in the keratoisidids, and since 2011, three new genera have been erected: *Cladarisis*, *Eknomisis*, and *Jasonisis*. The diversity within Keratoisididae has been described based on phylogenetic analysis [16], which found that the family has 11 genetically and morphologically distinct subclades with taxonomic characters such as sclerite composition (from the polyp body, tentacles, pharynx, and coenenchyme), gross colony morphology, polyp morphology, and polyp distribution along the axis used to discriminate among subclades. Half of the keratoisidid subclades do not contain any currently accepted genera, indicating the presence of many undescribed taxa within Keratoisididae. The genus *Chrysogorgia* is another taxonomically confusing group of octocorals. While it is one of the most abundant and diverse groups of octocorals, with 71 currently accepted species [17], recent investigations into the phylogenetic relationships among species within this genus have led to the proposal of 11 candidate genera [18], each of which has been assigned a group number in advance of formal description. There are fewer taxonomic problems within Primnoidae due to the work of dedicated museum taxonomists, unburdened by academic duties that university-based taxonomists face, and perhaps due to the frequent incorporation of genetics into their systematics, which helps test and reinforce the usefulness of certain taxonomic characters (e.g., [19–21]).

Coral gardens are widely distributed along the Irish continental slope and Rockall-Hatton Plateau, yet none of the known examples of calcaxonian-dominated coral gardens from Irish waters have had their main species fully identified (i.e., to species rank) despite the need for appropriate monitoring and reporting on their distributions. For example, of the three calcaxonian dominated coral gardens identified from Anton Dohrn seamount, the dominant bamboo coral is identified to genus rank in two biotopes (as *Keratoisis* sp. with *Solenosmilia variabilis* Duncan 1873 (Ker.Sol) in the first, and *Lepidisis* sp. with *Parantipathes*

sp. habitat (Lep.Par) in the other), and as an unidentified bamboo coral in a third (mixed coral dominated habitat comprising *S. variabilis*, *Anthomastus grandiflorus* Verrill 1878, an unidentified species of bamboo coral, and zoanthids (Gor.Zoa)) [22]. Similarly, in the Whittard Canyon, dense aggregations of “*Primnoa* sp.” have been reported from vertical walls ([23] Figure 3f).

Increased genomic resolution, provided by hundreds to thousands of single nucleotide polymorphisms (SNPs), is being used to successfully delimit species of octocorals [24–26], and SNPs can even detect the roles of hybridisation and introgression in species [27]. However, while next-generation sequencing costs are lowering, it is not cost-effective to generate whole-genome SNP data for exploratory studies that are investigating baseline information about the biodiversity present. Instead, DNA barcoding is commonly used, as it has overcome a lack of taxonomic knowledge in other groups by uncovering cryptic species diversity [28,29]. In octocorals, the usefulness of mitochondrial DNA barcoding is diminished due to the presence of an active mismatch repair gene, *mtMutS*, which reduces the accumulation of mutations in the mitochondrial genome [30,31]. However, while *mtMutS* itself is the most variable gene in the mitogenome [32,33], it is still insufficient to resolve species boundaries; therefore, a concatenated multilocus sequence (approximately 1648 bp long) consisting of *mtMutS* + *COI* + *igr1* and referred to as the “extended octocoral barcode” is widely used, although it is still not able to successfully delimit among all species due to a lack of interspecific variation associated with these genetic markers [34,35]. Within families, different gene regions have been used to further delimit species: *igr4* (the intergenic spacer between *COB* and *ND6*) has proved useful in Keratoisididae [36], while the addition of *ND2* to the extended octocoral barcode increased the number of successfully delimited species in the primnoid genus *Narella* [37].

The aims of this study were to (i) investigate the utility of a superextended barcode incorporating *mtMutS*, *COI* + *igr1*, 16S rRNA-*ND2*, and *igr4*, (ii) explore the effectiveness of various species delimitation techniques in successfully delimiting species in calcaxonian octocorals, and (iii) establish upper and lower bounds on the estimated number of calcaxonian species in Irish waters.

2. Materials and Methods

During two research surveys to the Irish Margin between 24 May–5 June 2017 and 11–23 August 2018 aboard *RV Celtic Explorer*, targeted collections of octocorals and sponges for biodiscovery gathered 70 Keratoisididae, 22 Primnoidae, 20 Chrysogorgiidae, and one Chelidonisididae (Table S1) using the robotic capabilities of *ROV Holland I*. All stations from 2017 were within the Whittard Canyon system between 1275 and 1988 m, except two located outside the Hovland Mound and Belgica Mound SACs at ~880 m, and stations from 2018 were within small canyons and gullies along the North Porcupine Bank between 821 and 2308 m (Figure 1).

Onboard, recovered specimens were kept in buckets of chilled seawater until processed. Genetic and morphological subsamples were taken and stored in 96% ethanol; remaining parts of specimens were stored dry at $-80\text{ }^{\circ}\text{C}$. Genetic subsamples comprised a few polyps of a coral and were stored in a 1.5-mL microcentrifuge tube. Morphological subsamples were approximately 4 cm in size and stored in glass vials.

All collected octocorals were photographed in situ using a Kongsberg OE14-208 Digital Still Camera attached to *Holland I* and again on board using a Nikon P900. The biodiscovery programme did not note the branching pattern (nodal vs. internodal vs. unbranched) of the bamboo corals (Families Keratoisididae and Chelidonisididae) or chrysogorgiids and the small morphological vouchers available for taxonomy usually did not contain a branching point. Branching pattern was not always evident in either in situ or ex situ photographs due to thick coenenchyme of bamboo corals or the bushy gross morphology of the chrysogorgiids.

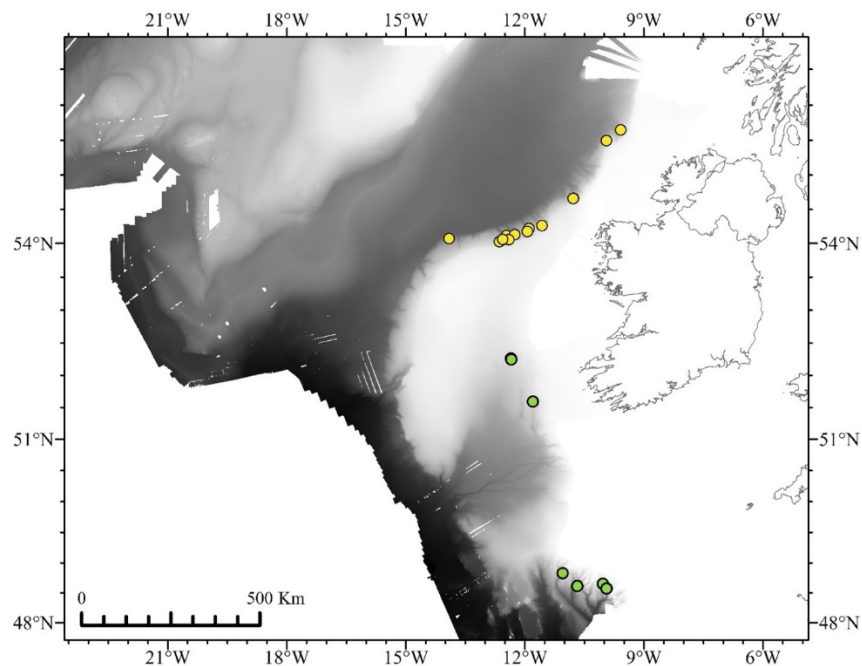


Figure 1. Locations of ROV dives that collected octocorals from 2017 (green circles) and 2018 (yellow circles). Bathymetry from INFOMAR and Ross et al. [38]. Visualized in ArcGIS Pro [39].

2.1. Genetics

2.1.1. DNA Extraction and Polymerase Chain Reaction (PCR)

Genomic DNA was extracted from individuals using a PureLink™ Genomic DNA Mini Kit (Invitrogen, Carlsbad, CA, USA) following the manufacturer's instructions. Partial regions of *mtMutS*, *COI* + *igr1*, *16S rRNA-ND2*, and *igr4* (*COB-ND6* intergenic spacer) were amplified for all individuals using PCR. Each 25 μ L PCR reaction contained 12.5 μ L of 1 \times GoTaq G2 Green Mastermix (Promega), 0.5 μ L of 10 μ M forward and reverse primers (final concentration 0.2 μ M), 9 μ L of nuclease free water, and 2.5 μ L of DNA template (<250 ng as per GoTaq G2 Green Mastermix protocol recommendations). Thermocycle profiles varied by primer pair (Table 1). PCR products were purified using a PureLink® PCR Purification kit (Invitrogen, Carlsbad, CA, USA) and sequenced with amplification primers in both forward and reverse directions by Eurofins Genomics.

2.1.2. DNA Sequence Quality Control, Haplotype Discovery, and Phylogenetic Inference

DNA sequences were assembled and amplification primers and poor quality bases were trimmed manually by examining chromatograms in Geneious Prime v. 2020.1.2 [40] and aligning the forward and reverse sequences using the pairwise alignment function to create a consensus sequence. Each genetic marker was aligned separately using the iterative refinement algorithm of MUSCLE [41] implemented in MEGA X [42] with default settings (Gap opening penalty of -400 , and no gap extension penalty). The intergenic spacer *igr4* and *COI* + *igr1* were also aligned using the L-INS-I iterative refinement alignment in MAFFT v. 7 [43] with default settings (Gap opening penalty of 1.5 and an offset value of 0.14) to account for the different indel placement by different alignment algorithms. Both methods yielded the same result. Sequences from coding regions were adjusted by eye so that codon-length gaps were in the correct position and did not change the amino acid sequence. Sequences from all targeted mitochondrial regions were concatenated into a 3390 bp alignment (hereafter referred to as the superextended barcode).

Table 1. Primer thermocycle profiles used to amplify mitochondrial gene fragment sequences.

Primer Name	Primer Sequences 5'–3'	Gene Boundaries Crossed	Thermocycle Profile	Source
CO3Bam5657f MUT3458R	GCT GCT AGT TGG TAT TGG CAT TSG AGC AAA AGC CAC TCC	CO3— <i>mtMutS</i>	^a 94 °C, 30 s: 55 °C, 30 s: 72 °C, 45 s. 35x or ^a 94 °C, 30 s: 55 °C, 60 s: 72 °C, 120 s. 35x	[44,45]
ND4L2475F MUT3458R	TAG GYT TAT TTA CTC ATA CWA T TSG AGC AAA AGC CAC TCC	ND4L— <i>mtMutS</i>	^b 94 °C, 20 s: 50 °C, 30 s: 72 °C, 50 s. 35x	[44,46]
COII8086f COIOCTr	CAT AAC AGG ACT AGC AGC ATC ATC ATA GCA TAG ACC ATA CC	COII— <i>igr1</i> — <i>COI</i>	^b 94 °C, 30 s: 47 °C, 30 s: 72 °C, 30 s. 40x	[34,47]
16s647F ND2_1417R	ACA CAG CTC GGT TTC TAT CTA CCA CAT CGG GGG CCC ACA TAT G	16S rRNA- <i>ND2</i>	^b 94 °C, 30 s: 47 °C, 30 s: 72 °C, 60 s. 30x	[47,48]
CytbBam1279f ND6Bam1648r	AGG AGC CAA TCC AGT AGA GGA ACC TAY AGG TAA GAA ATG CGA GTG ATC	COB- <i>ND6</i>	^b 94 °C, 30 s: 55 °C, 30 s: 72 °C, 45 s. 35x	[36]

^a Initial denaturing of DNA template at 94 °C for 5 min. Final extension 72 °C for 10 min. ^b Initial denaturing of DNA template 94 °C for 2 min. Final extension at 72 °C for 6 min.

Haplotypes from the concatenated alignment of the superextended barcode were recovered using TCS v 1.21 [49], which uses a statistical parsimony method. Statistical parsimony is defined as the connectivity between the most closely related haplotypes based on a user-defined probability [50]. Haplotypes will form a single network until the parsimony limit is reached. TCS allows gaps to be coded as a 5th character state, which allows indel variation and structure to be included in the analysis.

A Maximum Likelihood (ML) tree was constructed from haplotype sequences using IQ-Tree [51] with initial partitions between sequenced mitochondrial regions (*mtMutS*, *COI*, *igr1*, 16S rRNA, *ND2*, and *igr4*) and by first, second, and third codon positions in protein-coding genes (*mtMutS*, *COI*, and *ND2*). We used the settings -m MFP + Merge, which causes IQTree to implement PartitionFinder's greedy heuristic algorithm [52], to test whether partitions should be merged during the model selection. This heuristic algorithm merges partitions until the model fit does not increase further. IQTree retained three partitions (Table S2) and applied the TVM + F + R2 substitution model (transversion model where the A-G substitution rate equals the C-T substitution rate, with unequal base frequencies equivalent to the empirical base frequencies, and a FreeRate model with two rate categories) to the first partition and HKY + F + I (unequal transition/transversion rates and unequal base frequencies equivalent to the empirical base frequencies and a proportion of invariant sites) to the other two. Node support was determined using 1000 standard non-parametric bootstraps [53]. Nodes with support values lower than 70 were collapsed using TreeCollapseCL 4 (available at <http://hiv.bio.ed.ac.uk> (accessed on 10 May 2022)). A sequence from the species *Chelidonis aurantiaca* Studer, 1890 (Suborder Holaxonia; see [54]) was chosen as a suitable outgroup, as all ingroup specimens belonged to suborder Calcaxonia.

2.1.3. Genetic Species Delimitation

The widespread use of DNA barcoding across the tree of life has led to heuristic methods being developed to aid species delimitation. One of the first, and still one of the more popular methods, is the Automatic Barcode Discovery Gap [55], which uses pairwise genetic distances to identify a "barcode gap" which distinguishes intraspecific variation from species divergences. However, due to the slow mutating mitogenome of octocorals, many species share the same sequence across the genetic markers we have used, e.g., [34,35], meaning that in many cases there is no gap to discover. Therefore, this analysis was inappropriate for our data and was not conducted. The Generalized Mixed Yule Coalescent (GMYC) model is a tree-based method that uses phylogenetic information to find the transition between branching points based on coalescence within populations and Yule processes that are due to species divergence [56]. This is a maximum likelihood-based

method and requires an ultrametric tree. The results of the GMYC model are affected by phylogenetic uncertainty, thus a Bayesian implementation of this process (bGMYC) was developed that can incorporate this uncertainty and provide statistical probabilities [57]. Finally, “Poisson Tree Process” (PTP) methods use a rooted phylogenetic tree to identify speciation events based on the number of substitutions or branch lengths [58].

An ultrametric tree of all haplotypes was constructed with BEAST 2 [59] using the same partition scheme and substitution models found previously, an Optimised Relaxed Clock [60], and a Birth-Death tree prior (determined as best fit by AIC in comparison with the Yule model). The topology of the tree was constrained to that of the ML analysis by providing the ML tree as a starting tree and removing weight from those priors that affect tree topology. BEAST 2 searches were conducted with 10 million MCMC generations, with trees sampled every 1000 generations. A maximum clade credibility (MCC) tree annotated with median node ages in TreeAnnotator v2.6.3 summarised the posterior distribution of 9001 trees. The convergence of the MCMC runs and mixing of the chains were visually checked in Tracer v 1.6 by verifying the presence of a hairy-caterpillar-like trace. In addition, the effective sample size of all parameters was confirmed as above 200. An MCC tree annotated with median node age in TreeAnnotator v2.6.3 summarised the posterior distribution of 9001 trees.

The GMYC method [56] of species delimitation was implemented in the R package *Splits* [61], where both single (ST-GMYC) and multiple threshold (MT-GMYC) models were fitted on the MCC tree. A Bayesian extension of this model (bGMYC) was implemented in the R package bGMYC [57], with 50,000 MCMC steps including 40,000 as burn-in and a thinning of 100 steps. bGMYC accounts for uncertainty in the trees by sampling over a posterior distribution of randomly sampled trees; as input, one hundred randomly sampled trees were generated using LogCombiner v 2.6, which resampled the initial 9001 trees, generated from BEAST 2, at a lower frequency. We present the results for p (conspicuity among sequences) > 0.9 since $p > 0.95$ returns almost every terminus as a unique species, and we include results from different probability thresholds as a heatmap in supplementary information (Figure S50).

We also implemented the multi-rate Poisson Tree Processes (mPTP) method of delimitation using two runs of 10 million MCMC, sampling every 10,000 generations with a 20% burn-in. Both single (ST-mPTP) and multiple (MT-mPTP) threshold models were fitted.

2.2. Morphological Investigation

We examined the gross colony morphology from both the in situ and ex situ imagery (colony structure, branching frequency, polyp density, overall colony appearance) of every sample and assigned morphotype numbers to each unique morphology. We then grouped the samples by genetic haplotype and selected a representative coral specimen for detailed morphological examination for each morphotype present within each haplotype. Due to the limited tissue available for morphological analysis, we used a single polyp for SEM imaging, and a single polyp for in situ visualisation of sclerites. Characteristics such as polyp shape, position of the tentacles, composition, density, and orientation of the sclerites on the body were examined. We compared the findings of the gross morphology and SEM imaging to the relevant taxonomic literature to diagnose individuals to genus or species rank [62–70].

2.2.1. Light Microscopy Imaging and In Situ Sclerite Visualisation

Polyp morphology was examined using a dissecting microscope (Olympus ZXP16), and in situ sclerite arrangements of keratoisidids and chrysogorgiids: polyp body, tentacles, and coenenchyme were visualised by clearing the tissue for an hour in clove oil [16]. Once clear, polyps were examined while still submerged in clove oil between a pair of cross-polarising lenses, which reduces glare and reveals the birefringent properties of the sclerites. Images were taken with a camera (Olympus DP71) attached to the dissecting scope using extended focus and subsequently stacked using Combine ZP [71].

2.2.2. Scanning Electron Microscopy

Coral polyps were dissected to examine the different sclerite composition among the different anatomical parts of the coral (keratoisidids: polyp body, coenenchyme, tentacles, and pharynx, chrysogorgiids: polyp body, tentacles, and coenenchyme, primnoids: not dissected). The tissue from each part of the polyp was submerged separately in household bleach (5% sodium hypochlorite) for up to 1 hr to release sclerites, which were subsequently washed with distilled water (dH₂O) followed by 300 µL of 6% hydrogen peroxide. For the Primnoidae, the polyp was submerged whole in bleach under a microscope and sclerites were sorted (marginal, medial, basal, opercular, and tentacular sclerites). The reaction between sodium hypochlorite and hydrogen peroxide causes an effervescence that removes any remaining organic residues from the surface of the sclerites. A series of ten washes with dH₂O, three washes with 70% ethanol, and three washes in 100% ethanol ensured that sclerites were clean of organic debris and residual salts from the reaction between sodium hypochlorite and hydrogen peroxide. Using a 5x0 detail paintbrush/eyelash, sclerites were mounted onto a double-sided carbon adhesive fixed to a metal stub. Sclerites were gold coated for 120 s using a Quorum Q150R ESplus at a sputter current of 25 mA, resulting in a coat thickness of approximately 10 nm. If sclerites appeared charged during SEM imagery, an additional sputter coat using the same settings was applied and the sclerites reimaged. Sclerites were imaged at 15 kV using a Hitachi S-2600 at the Centre for Microscopy and Imaging, Anatomy, School of Medicine, National University of Ireland Galway. Qualitative descriptions of the sclerite shape and texture were noted and named according to the nomenclature established by Bayer et al. [72].

Keratoisidid polyp body, tentacle, pharynx, and coenenchyme sclerites were examined. Sclerites from the body, tentacles, and coenenchyme were examined from chrysogorgiids. Body wall and opercular scales, in addition to coenenchyme and tentacle sclerites, were examined from specimens of Primnoidae.

2.3. Taxon Identification and Nomenclature Used throughout This Study

Sequences of *mtMutS* generated in this study (Table 2) were compared with those on GenBank using BLAST to provide a family-level indication of taxon identity.

Specimens were initially identified as bamboo corals based on the occurrence of proteinaceous nodes in an otherwise calcareous skeleton, and their placement in the Keratoisididae was confirmed by amplifying across the CO3—*mtMutS* gene boundary, an arrangement only found in Keratoisididae and some species of *Anthoptilum* sea pens [73]. For Keratoisididae, we labelled our tree termini with the subclade nomenclature established by France [14] and expanded by Watling et al. [16]. We assigned the nomenclature based on *mtMutS* sequences generated in this study that were identical or extremely similar (>99.5%) to keratoisidid *mtMutS* sequences used in Watling et al. [16]. Individuals in the genus *Chrysogorgia* s.l. were assigned, on the basis of morphological characteristics, by co-author CBU to the established groups of Untiedt et al. [18] to better quantify the observed diversity within the genus while it is undergoing a major redescription. We were conservative in our identifications, and only identified individuals to genus and/or species when we were confident that characteristics matched the relevant taxonomic literature [62–70]. Where there was doubt, we assigned individuals to a higher taxonomic rank in which we had confidence.

Table 2. GenBank Accession numbers for gene fragments sequences for every morphotype.

Specimen Voucher	USNM Number	Specimen ID	Haplotype/Morphotype	mtMutS	COI + igr1	16s rRNA-ND2	igr4
CE-17-266	1593468	Keratoisididae D1 sp.	1/7	ON971007	ON971056	ON971105	ON971154
CE-18-646	1593473	Keratoisididae D1 sp.	1/8	ON971008	ON971057	ON971106	ON971155
CE-18-508	1593474	Keratoisididae D1 sp.	2/9	ON971009	ON971058	ON971107	ON971156
CE-17-269	1593475	Keratoisididae B1 sp.	3/12	ON971010	ON971059	ON971108	ON971157
CE-17-174	1593476	Keratoisididae B1 sp.	4/10	ON971011	ON971060	ON971109	ON971158
CE-17-206	1593477	Keratoisididae B1 sp.	5/13	ON971012	ON971061	ON971110	ON971159
CE-17-146	1593481	Keratoisididae B1 sp.	6/10	ON971013	ON971062	ON971111	ON971160
CE-17-424	1593483	Keratoisididae B1 sp.	6/11	ON971014	ON971063	ON971112	ON971161
CE-17-201	1593489	<i>Eknomisis</i> sp.	7/4	ON971015	ON971064	ON971113	ON971162
CE-18-129	1593490	<i>Eknomisis</i> sp.	8/5	ON971016	ON971065	ON971114	ON971163
CE-18-387	1593492	<i>Eknomisis</i> sp.	8/6	ON971017	ON971066	ON971115	ON971164
CE-18-288	1593493	Keratoisididae D2 sp.	9/1	ON971018	ON971067	ON971116	ON971165
CE-17-222	1593498	Keratoisididae D2 sp.	10/3	ON971019	ON971068	ON971117	ON971166
CE-18-039	1593495	Keratoisididae D2 sp.	11/2	ON971020	ON971069	ON971118	ON971167
CE-18-203	1593497	Keratoisididae I1 sp.	12/15	ON971021	ON971070	ON971119	ON971168
CE-17-234	1593498	Keratoisididae I1 sp.	13/16	ON971022	ON971071	ON971120	ON971169
CE-18-063	1593499	Keratoisididae I1 sp.	13/17	ON971023	ON971072	ON971121	ON971170
CE-18-415	1593500	Keratoisididae I1 sp.	13/18	ON971024	ON971073	ON971122	ON971171
CE-18-110	1593503	Keratoisididae I1 sp.	14/17	ON971025	ON971074	ON971123	ON971172
CE-17-125	1593509	Keratoisididae I1 sp.	15/19	ON971026	ON971075	ON971124	ON971173
CE-17-287	1593512	Keratoisididae C1 sp.	16/28	ON971027	ON971076	ON971125	ON971174
CE-18-242	1593514	Keratoisididae C1 sp.	16/29	ON971028	ON971077	ON971126	ON971175
CE-17-356	1593516	Keratoisididae C1 sp.	17/30	ON971029	ON971078	ON971127	ON971176
CE-17-276	1593517	Keratoisididae J3 sp.	18/20	ON971030	ON971079	ON971128	ON971177
CE-17-274	1593518	Keratoisididae J3 sp.	19/21	ON971031	ON971080	ON971129	ON971178
CE-18-538	1593524	Keratoisididae J3 sp.	19/22	ON971032	ON971081	ON971130	ON971179
CE-17-367	1593526	Keratoisididae J3 sp.	20/23	ON971033	ON971082	ON971131	ON971180
CE-17-304	1593531	<i>Acanella arbuscula</i>	21/24	ON971034	ON971083	ON971132	ON971181
CE-17-357	1593535	<i>Acanella arbuscula</i>	21/25	ON971035	ON971084	ON971133	ON971182
CE-17-425	1593532	<i>Acanella arbuscula</i>	21/26	ON971036	ON971085	ON971134	ON971183
CE-18-339	1593536	<i>Acanella</i> sp.	22/27	ON971037	ON971086	ON971135	ON971184
CE-17-216	1593537	Keratoisididae F1 sp.	23/14	ON971038	ON971087	ON971136	ON971185
CE-17-181	1593580	<i>Chelidonisis aurantiaca</i>	24/44	ON971039	ON971088	ON971137	ON971186
CE-17-364	1593538	<i>Chrysogorgia</i> Group 7 sp.	25/37	ON971040	ON971089	ON971138	ON971187
CE-17-271	1593539	<i>Chrysogorgia</i> Group 7 sp.	26/38	ON971041	ON971090	ON971139	ON971188
CE-17-129	1593543	<i>Chrysogorgia</i> Group 3 sp.	27/39	ON971042	ON971091	ON971140	ON971189
CE-17-283	1593545	<i>Chrysogorgia</i> Group 3 sp.	27/40	ON971043	ON971092	ON971141	ON971190
CE-18-292	1593548	<i>Chrysogorgia</i> Group 3 sp.	27/41	ON971044	ON971093	ON971142	ON971191
CE-18-418	1593551	<i>Dasygorgia</i> sp.	28/42	ON971045	ON971094	ON971143	ON971192
CE-18-237	1593554	<i>Chrysogorgia</i> Group 1 sp.	29/43	ON971046	ON971095	ON971144	ON971193
CE-18-434	1593558	<i>Narella bellissima</i>	30/32	ON971047	ON971096	ON971145	ON971194
CE-17-290	1593559	<i>Candidella imbricata</i>	31/34	ON971048	ON971097	ON971146	ON971195
CE-18-321	1593564	<i>Narella versluysi</i>	32/33	ON971049	ON971098	ON971147	ON971196
CE-17-095	1593566	<i>Primnoa</i> sp.	33/31	ON971050	ON971099	ON971148	ON971197
CE-17-160	1593567	<i>Primnoa</i> sp.	34/31	ON971051	ON971100	ON971149	ON971198
CE-17-082	1593568	<i>Primnoa</i> sp.	35/31	ON971052	ON971101	ON971150	ON971199
CE-17-101	1593572	<i>Primnoa</i> sp.	36/31	ON971053	ON971102	ON971151	ON971200
CE-18-261	1593574	<i>Thouarella grasshoffi</i>	37/35	ON971054	ON971103	ON971152	ON971201
CE-18-568	1593579	<i>Calyptraphora clinata</i>	38/36	ON971055	ON971104	ON971153	ON971202

3. Results

Sequencing revealed 38 unique sequences (haplotypes, H1–H38; Table S3) from the concatenated alignment of the superextended barcode representing 44 distinct morphotypes, numbered M1–M44 (Figures 2–5 and S1–S49). More haplotypes were recovered using the superextended barcode than with each genetic marker independently (Table S3). In the ML tree, three main clades, each with bootstrap support of 100%, represented (1) Keratoisididae, (2) Primnoidae, and (3) Chrysogorgiidae (Figure 6). All specimens were deposited at the Smithsonian Institution National Museum of Natural History Invertebrate Collection (USNM: 159348–1593580, Table S1).

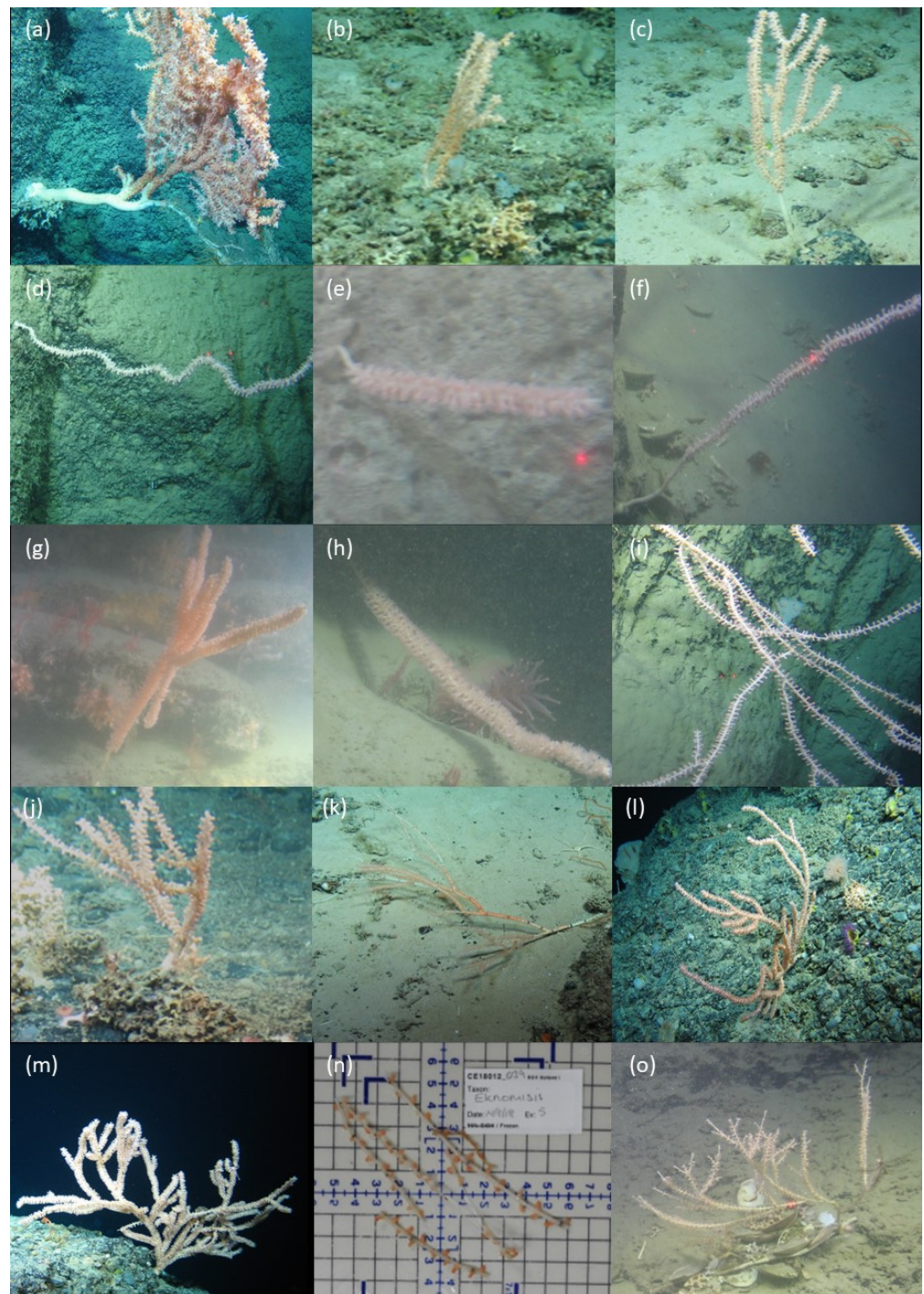


Figure 2. In situ photographs taken by ROV *Holland I* representing the gross morphology of (a) Haplotype 1 (M7), (b) Haplotype 1 (M8), (c) Haplotype 2 (M9), (d) Haplotype 3 (M12), (e) Haplotype 4 (M10), (f) Haplotype 5 (M13), (g) Haplotype 6 (M10), (h) Haplotype 6 (M11), (i) Haplotype 7 *Eknomisis* sp. (M4), (j) Haplotype 8 *Eknomisis* sp. (M5), (k) Haplotype 8 *Eknomisis* sp. (M6), (l) Haplotype 9 (M1), (m) Haplotype 10 (M3), (n) Haplotype 11 (M2)(there was no in situ image found of Haplotype 11, instead there is an image taken in the laboratory) and (o) Haplotype 12 (M15).

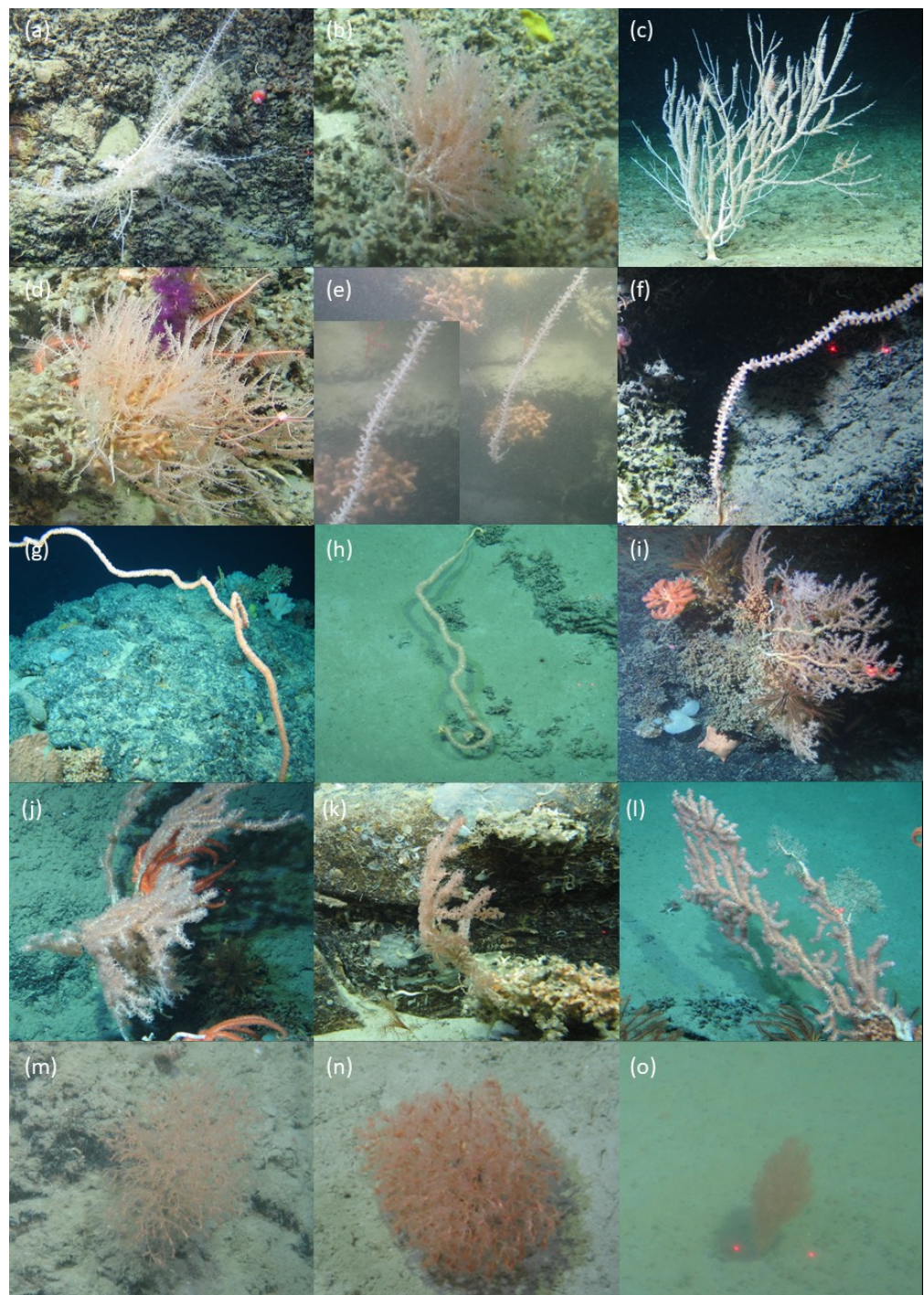


Figure 3. In situ photographs taken by ROV *Holland I* representing the gross morphology of (a) Haplotype 13 (M16), (b) Haplotype 13 (M17), (c) Haplotype 13 (M18), (d) Haplotype 14 (M17), (e) Haplotype 15 (M19), (f) Haplotype 16 (M28), (g) Haplotype 16 (M29), (h) Haplotype 17 (M30), (i) Haplotype 18 (M20), (j) Haplotype 19 (M21), (k) Haplotype 19 (M22), (l) Haplotype 20 (M23), (m) Haplotype 21 *Acanella arbuscula* (M24), (n) Haplotype 21 *A. arbuscula* (M25), and (o) Haplotype 21 *A. arbuscula* (M26).

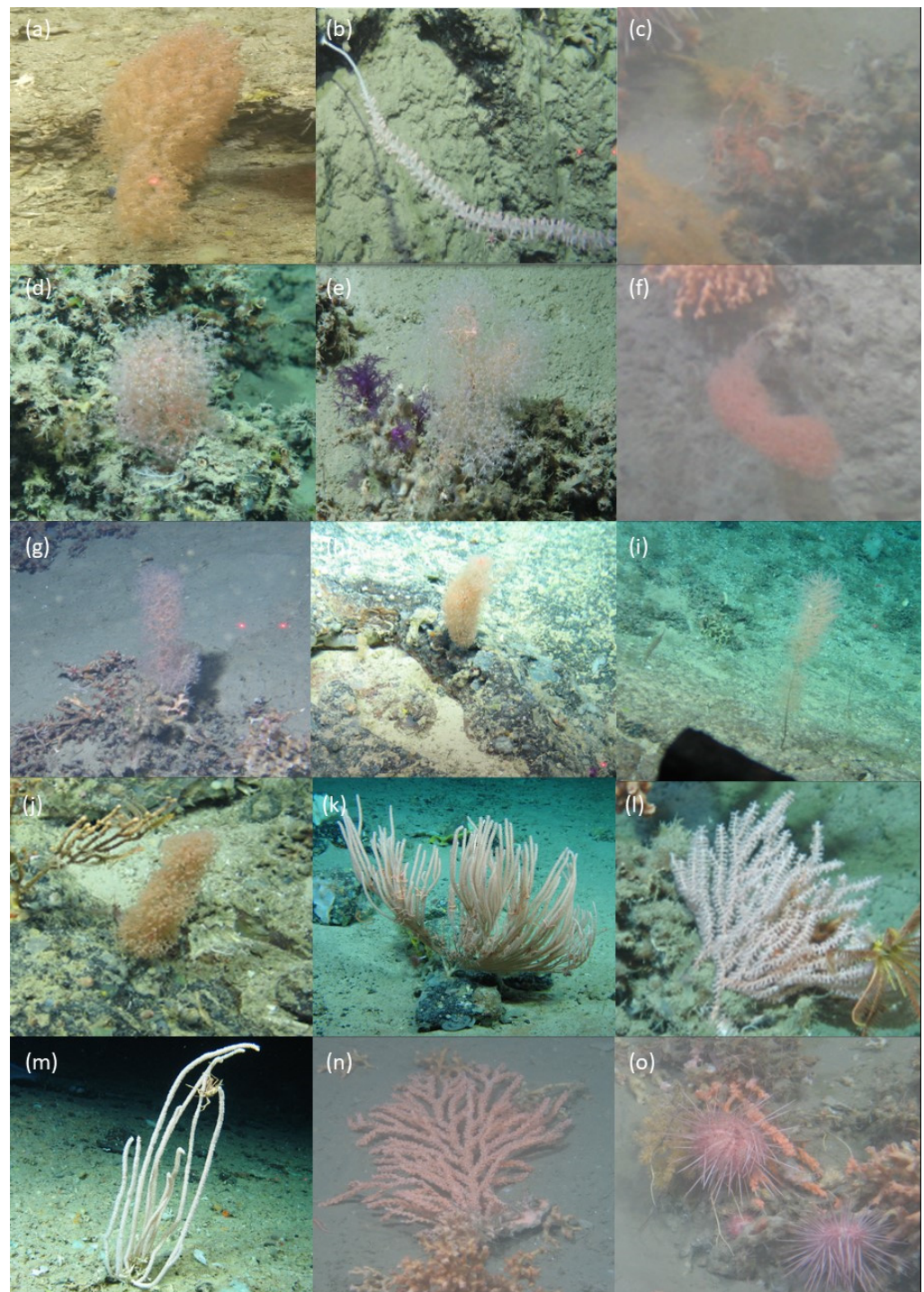


Figure 4. In situ photographs taken by ROV *Holland I* representing the gross morphology of (a) Haplotype 22 *Acanella* sp. (M27), (b) Haplotype 23 (M14), (c) Haplotype 24 *Chelidonis aurantiaca* (M44), (d) Haplotype 25 *Chrysogorgia* s.l. Group 7 (M37), (e) Haplotype 26 *Chrysogorgia* s.l. Group 7 (M38), (f) Haplotype 27 *Chrysogorgia* s.l. Group 3 (M39), (g) Haplotype 27 *Chrysogorgia* s.l. Group 3 (M40), (h) Haplotype 27 *Chrysogorgia* s.l. Group 3 (M41), (i) Haplotype 28 *Dasygorgia* (M42), (j) Haplotype 29 *Chrysogorgia* s.l. Group 1 (M43), (k) Haplotype 30 *Narella bellissima* (M32), (l) Haplotype 31 *Candidella imbricata* (M34), (m) Haplotype 32 *Narella versluysi* (M33), (n) Haplotype 33 *Primnoa* sp. (M31) and (o) Haplotype 34 *Primnoa* sp. (M31).

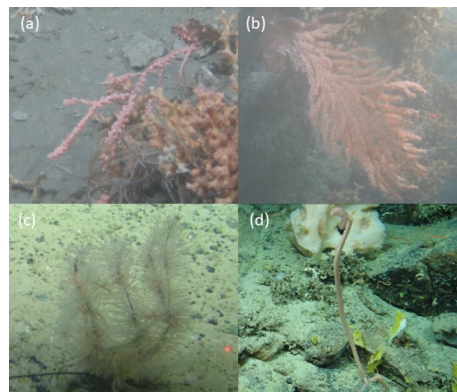


Figure 5. In situ photographs taken by ROV *Holland I* representing the gross morphology of (a) Haplotype 35 *Primnoa* sp. (M31), (b) Haplotype 36 *Primnoa* sp. (M31), (c) Haplotype 37 *Thouarella grasshoffi* (M35), and (d) Haplotype 38 *Calyptrophora clinata* (M36).

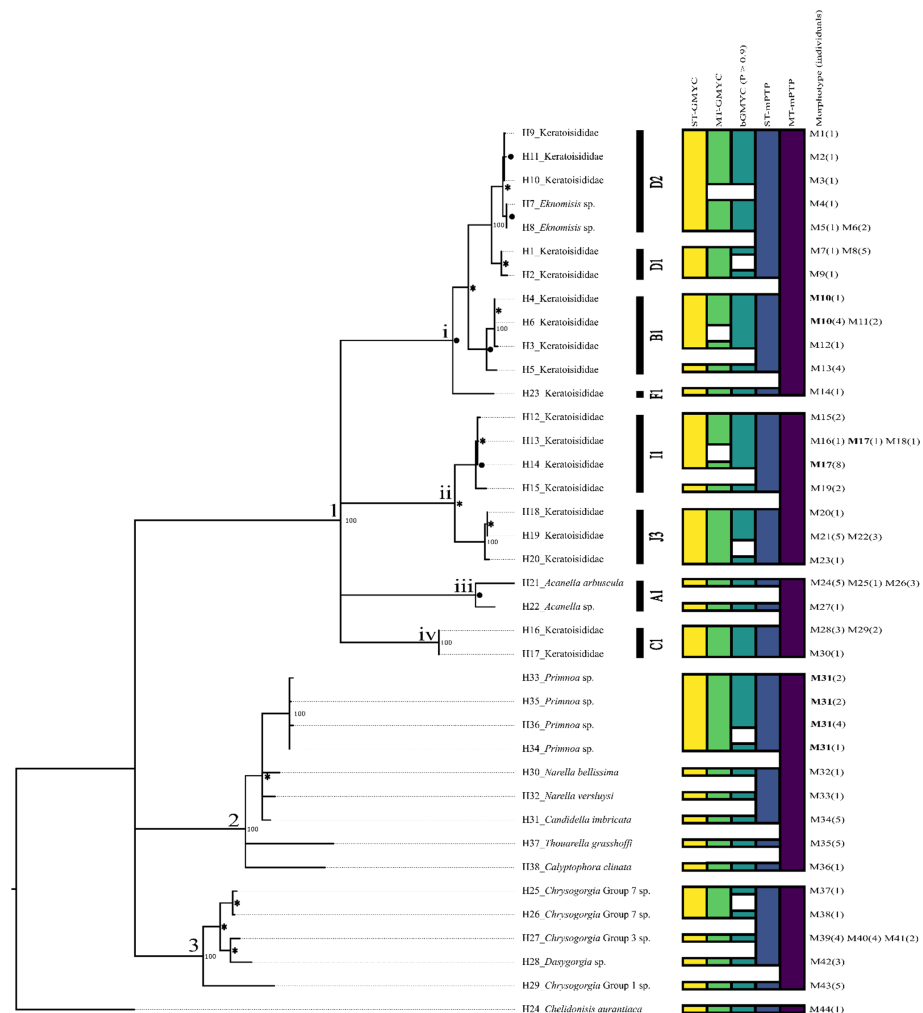


Figure 6. Maximum likelihood tree of all recovered haplotypes (H) and corresponding morphotypes (M) from the 3390 base pair alignment and the corresponding species delimitation results from GMYC and mPTP methods (ST = single threshold and MT = multiple threshold). Each box within each column refers to a unique species recovered by that method. 1. Family Keratoisididae. A1, B1, C1, D1, D2, F1, I1, and J3 refer to the keratoisidid subclades defined by Watling et al. [16], 2. Family Primnoidae, and 3. Family Chrysogorgiidae. * represent bootstrap values 90–99. • represents bootstrap values between 71–89. Nodes with support lower than 70 have been collapsed and bootstrap values not displayed.

3.1. Clade 1—*Keratoisididae*

Gross morphology identified 30 keratoisidid morphotypes belonging to 23 haplotypes. The primary morphological features (colony shape, branching pattern, polyp morphology, coenenchyme thickness, tentacle positioning, and sclerome) of each morphotype are summarised in Table 3.

Genus names could be assigned to some haplotypes identified as being members of Watling et al.'s [16] subclades A1 (*Acanella*) and D2 (*Eknomisis*). The subclades B1, C1, D1, and F1 do not contain any currently accepted genera, and the only recognised genus to date in I1 is *Lepidisis*. *Lepidisis* is polyphyletic [74], as lack of branching is the diagnostic characteristic for this genus, and this trait is now recognised as labile [14,15,75]. Thus, *Lepidisis* cannot be used to broadly diagnose unbranched bamboo corals, and the true generic affinity of nine of the eleven presently accepted species is uncertain (see [74]). Only *Lepidisis caryophyllia* Verrill, 1883 (the type species) and *Lepidisis cyanae* Grasshoff, 1986 are considered to be representatives of the genus. None of our specimens matched the type description of *L. cyanae* (the polyp morphology and sclerite composition is best observed in Figures 8 and 9 in Grasshoff [76]), which is known to occur in the Northeast Atlantic. *Jasonisis* is the only accepted genus recognised from J3. No individuals within J3 in our study could be diagnosed as representative of that genus. It is known that there are many undescribed genera within *Keratoisididae* [16], thus, in many cases, there are no names to assign.

Keratoisididae (Clade 1) is composed of four smaller clades (1i, 1ii, 1iii, and 1iv) joined in a polytomy.

Clade 1i, which unites 12 termini, received 85% bootstrap support and contains representatives of the France/Watling [16] subclades D2, D1, B1, and F1. One species delimitation method, MT-mPTP, recovered this entire clade as a single species.

Members of D1 and D2 were recovered in a monophyletic group (100% bootstrap support) comprising 14 individuals. ST-mPTP species delimitation recovered these seven haplotypes as a single species. Of these seven haplotypes, five (Haplotypes 7, 8, 9, 10, and 11) belonged to D2. MT-GMYC and ST-mPTP recovered these five haplotypes as a single species, but MT-GMYC and bGMYC recognised Haplotypes 9, 10, and 11 as one species and Haplotypes 7 and 8 as a second. Haplotypes 7 and 8 were identified as representatives of the genus *Eknomisis* due to the oblique arrangement of the needle and rod sclerites along the polyp body (Figures S4–S6) [68].

Two haplotypes belonged to D1 (Haplotype 1 and 2) and were recovered as sister species (93% bootstrap support). Both ST- and MT-GMYC recognized the two haplotypes as one species; only bGMYC recognised these two haplotypes as individual species.

Fourteen individuals belonging to four haplotypes (Haplotype 3–Haplotype 6) were considered as representative of Watling et al.'s [16] B1 and were unified with 72% bootstrap value. ST-GMYC and bGMYC recognised Haplotype 3, Haplotype 4, and Haplotype 6 as one species, with Haplotype 5 as a second, whereas ST-mPTP recognised all four haplotypes as one species, and MT-GMYC recognised three species, uniting Haplotype 4 and Haplotype 6 as one of those three species. Among the fourteen individuals, five morphotypes were discerned (Table 3).

Lineage F1 (Haplotype 23, Figure 4b) is represented by a single whip coral. All species delimitation methods recovered this haplotype as representing a single species except MT-mPTP, which considered this lineage to be part of a species also encompassing B1, D1, and D2.

Clade 1ii comprises representatives of Watling et al. [16] subclades I1 and J3, with seven termini unified by a node with 99% bootstrap support. One species delimitation method, MT-mPTP, determined the entire clade was representative of only a single species.

Table 3. Key morphological characteristics of the Keratoisididae morphotypes.

Morphotype (Haplotype, Figures)	Designation	Colony Shape	Branching	Polyp Morphology	Coenenchyme	Tentacles	Polyp Body Sclerites	Tentacle Sclerites	Pharynx Sclerites	Coenenchyme Sclerites
1 (9; Figure 2i and Figure S1)	Keratoisididae D2 sp.	Planar	Sparse dichotomous, internodal	Cylindrical. Originate from all sides of coenenchyme	Thick. Cream to pink	In the oral area	Needles arranged longitudinally	Blunt ended rods Needles	Thorned rodlets	Needles
2 (11, Figure 2n and Figure S2)	Keratoisididae D2 sp.	Unknown	Unknown	Orange	Unknown	Folded over mouth	Rods arranged obliquely and longitudinally	Blunt ended rods and flattened rods	Unknown	Rods
3 (10, Figure 2m and Figure S3)	Keratoisididae D2 sp.	Arborescent	Frequent dichotomous, internodal	Cylindrical. Orange to pink. Originate on all sides of coenenchyme	Thick	In the oral area	Needles and rods arranged longitudinally	Blunt ended rods and flattened rods	Thorned rodlets	Needles and rods
4 (7, Figure 2i and Figure S4)	<i>Eknomisis</i> sp.	Arborescent	Sparse dichotomous, internodal	Distally tapered. Pink Originate in two planes?	Thin	In the oral area	Rods arranged obliquely	Blunt ended rods and flattened rods	Thorned rodlets	Rods
5 (8, Figure 2j and Figure S5)	<i>Eknomisis</i> sp.	Arborescent	Sparse dichotomous, internodal	Distally tapered. Pink Originate on all sides of coenenchyme	Thin	In the oral area	Needles and rods arranged obliquely	Blunt ended rods and flattened rods	Thorned rodlets	Rods
6 (8, Figure 2k and Figure S6)	<i>Eknomisis</i> sp.	Arborescent	Sparse dichotomous, internodal	Barrel shaped.	Thin	Folded over mouth	Needles and rods arranged obliquely	Blunt ended rods and flattened rods	Thorned rodlets	Needles and rods
7 (1, Figure 2a and Figure S7)	Keratoisididae D1 sp.	Planar	Frequent dichotomous, internodal	Pink to orange. Cylindrical.	Thick	In the oral area	Needles and rods arranged obliquely and longitudinally	Blunt ended rods and flattened rods	Thorned rodlets	Unknown
8 (1, Figure 2b and Figure S8)	Keratoisididae D1 sp.	Arborescent	Sparse dichotomous, internodal	Pink to orange. Cylindrical. Originate on all sides of coenenchyme	Thick	In the oral area	Needles and rods arranged obliquely	Blunt ended rods and flattened rods	Thorned rodlets	Unknown
9 (2, Figure 2c and Figure S9)	Keratoisididae D1 sp.	Planar	Sparse dichotomous, internodal	Pink to orange. Cylindrical. Originate on all sides of coenenchyme	Thin	In the oral area	Needles and rods arranged obliquely	Blunt ended rods and flattened rods	Thorned rodlets	Unknown
10 (4, Figure 2e and Figure S10)	Keratoisididae B1 sp.	Whip or planar	Branched and unbranched forms	Trumpet shape. Originate on all sides of coenenchyme	Thick	Folded over mouth	Needles and scales arranged obliquely and longitudinally	Flattened rods	Thorned rodlets	Needles and scales
10 (6, Figure 2g and Figure S11)	Keratoisididae B1 sp.	Whip or planar	Branched and unbranched forms	Trumpet shaped. Originate on all sides of coenenchyme	Thick	Folded over mouth	Needles and scales arranged obliquely and longitudinally	Elongated, narrow flattened rods	Thorned rodlets	Needles and scales

Table 3. Cont.

Morphotype (Haplotype, Figures)	Designation	Colony Shape	Branching	Polyp Morphology	Coenenchyme	Tentacles	Polyp Body Sclerites	Tentacle Sclerites	Pharynx Sclerites	Coenenchyme Sclerites
21 (19, Figure 3j and Figure S23)	Keratoisididae J3 sp.	Planar	Branched	Trumpet shaped, originating from all sides of the coenenchyme Taper distally, originating from all sides of the coenenchyme	Thick	Folded over mouth	Spindles and rods arranged longitudinally	Flattened rods	Flattened rods	Spindles and Needles
22 (19, Figure 3k and Figure S24)	Keratoisididae J3 sp.	Planar	Di- and trichotomous, nodal	Barrel shaped, originating from all sides of the coenenchyme	Thin	In the oral area	Rods arranged obliquely and longitudinally	Flattened rods	Flattened rods	Rods
23 (20, Figure 3l and Figure S25)	Keratoisididae J3 sp.	Planar	Dichotomous, nodal	Barrel shaped, originating from all sides of the coenenchyme	Thick	Folded over mouth	Needles and rods arranged longitudinally	Flattened rods	Sparsely toothed rods	Rods, flattened rods
24 (21, Figure 3m and Figure S26)	<i>Acanella arbuscula</i>	Loose bush	Sparse di- and trichotomous, nodal	Funnel shaped	Thin	Folded over mouth	Rods arranged obliquely	Rods and flattened rods	Elongated thorny rods	Rods
25 (21, Figure 3n and Figure S27)	<i>Acanella arbuscula</i>	Tight bush	Nodal	Slender, same width throughout	Thin	Folded over mouth	Needles arranged obliquely	Rods and flattened rods	Rod	Rods
26 (21, Figure 3o and Figure S28)	<i>Acanella arbuscula</i>	Funnel shaped bush	Sparse di- and trichotomous, nodal	Barrel shaped	Thin, thickening distally	Folded over mouth	Needles arranged obliquely	Rods and flattened rods	Elongated thorny rods	Rods
27 (22, Figure 4a and Figure S29)	<i>Acanella</i> sp.	Fan/bush	dichotomous, nodal	Barrel	Thin, thickening distally	Contracted over mouth	Rods and needles arranged obliquely	Rods and flattened rods	Elongated thorny rods	Needles and rods
28 (16, Figure 3f and Figure S30)	Keratoisididae C1 sp.	Whip	Unbranched	Barrel shaped, originate on all sides	Thick	Folded over mouth	Sparse, needles, arranged obliquely and longitudinally	Flattened rods	Elongated diamond rods	Unknown
29 (16, Figure 3g and Figure S31)	Keratoisididae C1 sp.	Whip	Unbranched	Barrel shaped, originate on all sides	Thick	Folded over mouth	Sparse, needles, arranged obliquely and longitudinally	Flattened rods	Elongated diamond rods	Needles and elongated rods
30 (17, Figure 3h and Figure S32)	Keratoisididae C1 sp.	Whip	Unbranched	Barrel shaped, originate on all sides	Thick	Folded over mouth	Sparse, needles, arranged obliquely	Flattened rods	Elongated diamond rods	Rods and flattened rods

Subclade I1 has four termini (Haplotypes 12–15) united by 86% bootstrap support. Both ST- and MT-mPTP recovered the four haplotypes as one species, but other genetic species delimitation methods generated different solutions: ST-GMYC and bGMYC united Haplotype 12–Haplotype 14 as a species, but delimited Haplotype 15 as a unique species while MT-GMYC united Haplotype 12 and Haplotype 13, but delimited each of Haplotype 14 and Haplotype 15 as unique species. The fifteen specimens whose sequences formed subclade I1 comprised five morphotypes (Table 3).

Subclade J3 has three termini (Haplotypes 18–20), comprising ten individuals (representing four morphotypes) united with 100% bootstrap support. These three haplotypes were recovered as a single species by all genetic species delimitation methods except bGMYC, which combined Haplotype 18 and Haplotype 19 as a single species, and recovered Haplotype 20 as a separate unique species. The tissue of every one of our individuals assigned to J3 turned various shades of brown post-preservation in 100% ethanol, a process that has only been reported in keratoisidids for the species *Jasonisis thresheri* Alderslade and McFadden, 2012 [77] but occurs in other J3 specimens (*pers. obs.* D. Morrissey), suggesting this may be a useful diagnostic trait of the wider J3 subclade.

Clade Iiii unites two termini, both of which are representative of Watling et al. [16] subclade A1, with 73% bootstrap support. MT-mPTP recovered this clade and clade Iiv as a single species.

Subclade A1 contains two termini (Haplotypes 21 and 22), which were consistently delimited as separate species by all genetic species delimitation methods except ST-mPTP. The ten specimens which yielded these two haplotypes were diagnosed as *Acanella* based on the orange-coloured bush-like colonies which branch from the nodes in whorls. The three morphotypes of specimens sequenced as Haplotype 21 varied from loose to tightly branched bushes (M24, Figure 3m; M25, Figure 3n; and M26, Figure 3o), with M24 being found in deeper water (~2000 m), M26 in shallower water (~1300 m), and M25 in intermediate depths (~1600 m). M24, M25, and M26 were all identified as *Acanella arbuscula* due to the funnel-shaped polyps and/or the presence of elongated rods arranged obliquely along the polyps (Figures S26–S28) [69]. The single specimen sequenced as Haplotype 22 has a flattened more planar colony form (M27, Figure 4a) that does not match the description of any accepted species of *Acanella* known from the North Atlantic [69]. However, it is possible that this specimen is also *A. arbuscula* and that the full range of intraspecific variation of this species has yet to be described. Due to the current taxonomic uncertainty, the assignment was left at genus rank.

Clade Iiv contains only individuals assigned to Watling et al. (2022) subclade C1. Subclade C1 contained two termini (Haplotype 16 and 17), which were each recovered as a species by all genetic species delimitation methods except MT-mPTP, which recovered Clade Iiv and Clade Iiii as a single species. C1 specimens comprised three morphotypes of unbranched whip corals (Table 3).

3.2. Clade 2—Primnoidae

Primnoidae was recovered as monophyletic (Clade 2), comprising nine haplotypes (Haplotypes 31–38) unified by a node with 100% bootstrap support. According to genetic species delimitation methods, these termini represented as many as seven species, or as few as one (Table 4). Species names were assigned to all primnoid haplotypes except the four haplotypes assigned to *Primnoa* sp. (H33–H36). All *Primnoa* sp. haplotypes were united with 100% bootstrap support. All genetic species delimitation methods recognized these four haplotypes as a single species, except for bGMYC, which recognised Haplotype 34 as one species and Haplotypes 33, 35, and 36 as another, and MT-mPTP, which, while recognising the four termini as one species, also included five other termini as representing that species. All *Primnoa* sp. haplotypes comprised a single shared morphotype (M31) which had a similar gross morphology to *Primnoa resedaeformis* (Gunnerus, 1763), including an arborescent colony form densely packed with irregularly placed polyps. However, there were key characteristics differentiating the morphotype from *P. resedaeformis*: M31 had

neatly arranged paired abaxial body–wall scales (Figures S33–S36), while the body–wall scales of *P. resedaeformis* are characteristically irregularly placed (best observed in Figure 2 of Cairns and Bayer [65]). A wide variation in polyp morphology has been reported for *P. resedaeformis* [65], which could mean that the morphological differences observed in M31 could be attributed to intraspecific variation; however, since we could not confidently determine this, the assignment of M31 was kept at genus rank.

Table 4. Upper and lower bounds of the potential number of species per family. See Section 3.5 for the justification and reasoning for each estimate.

Family	Lower Bound of Species Estimate	Upper Bound of Species Estimate
Keratoisididae	14	27
Primnoidae	6	7
Chrysogorgiidae	4	5
Chelidonisididae	1	1
Total	25	40

In a larger clade with *Primnoa* sp. are *Narella bellissima* (Kükenthal, 1915), *Narella versluysi* (Hickson, 1909), and *Candidella imbricata* (Johnson, 1862) (Haplotypes 30–32), unified by 93% bootstrap support. *Narella bellissima* was identified by its distinctive lyrate branching (M32, Figure 4k) and the presence of larger yet fewer polyps per whorl. *Narella versluysi* was identified by its sparsely dichotomous branching (M33, Figure 4m) and smaller, more densely packed polyps per whorl. *Candidella imbricata* was identified by the characteristic fan shape of the parent colony that had polyps standing perpendicular to the main axis (M34, Figure 4l). ST-GMYC, MT-GMYC, and bGMYC identified those as three separate species, whereas ST-mPTP identified them as a single species, and MT-mPTP identified them as components of a single species that spans Clade 2.

The remaining two termini of Clade 2 were identified as *Thouarella grasshoffi* Cairns, 2006 (Haplotype 37) and *Calyptraphora clinata* Cairns, 2007 (Haplotype 38). *Thouarella grasshoffi* is one of only two *Thouarella* species in the North Atlantic and is distinctive due to its bottle-brush colony morphology (M35, Figure 5c) and the presence of paired polyps. *Calyptraphora clinata* has downward-facing polyps, with the basal scales containing a pair of thin spines that are serrated along their entire length (M36, Figure 5d). All genetic delimitation methods recovered these as unique species, except for MT-mPTP, which recovered a single species for the entire Primnoidae clade (Clade 2), as mentioned previously.

3.3. Clade 3—*Chrysogorgiidae*

Five haplotypes (Haplotypes 25, 26, 27, 28, and 29), were recovered within a monophyletic clade. All 20 individuals were initially assigned to the genus *Chrysogorgia* s.l. Duchassaing and Michelotti, 1864 due to the distinctive overall colony morphologies and results from comparisons of *mtMutS* in GenBank. One of the authors (CBU) identified individuals based on taxonomically useful morphological characters to their corresponding new group ID, as established in Untiedt et al. [18]. Haplotype 27 was assigned to Group 3 (M39–M41), Haplotype 28 was assigned to *Dasygorgia* (M42, Figure 4i), Haplotype 29 was assigned to Group 1 (M43, Figure 4j), and Haplotype 25 (M37, Figure 4d) and Haplotype 26 (M38, Figure 4e) were assigned to Group 7. M39 and M41, represented by four and two individuals, respectively, both had a bottle brush gross colony shape. M39 was orange in colour, with an unbranched axial skeleton (main stem of the coral) and a dense population of polyps on the lateral branches such that the main stem was not visible. M41, had a distinctive “Y” branching at the distal end of the main stem and lateral branches containing fewer polyps. M40 comprised two individuals with unbranched axial skeletons with pinker, well-spaced polyps along the lateral branches resulting in an overall colony morphology reminiscent of a small loose bush.

All delimitation methods except bGMYC found both representatives of Group 1 (Haplotype 25 and Haplotype 26) to be the same species, and all GMYC methods (ST-GMYC, MT-GMYC, bGMYC) found that Haplotype 27, Haplotype 28, and Haplotype 29 each represent a distinct species. ST-mPTP delimited two species, one represented by Haplotypes 25–28 and the other by Haplotype 29, while MT-mPTP recovered the clade as a single species.

3.4. *Chelidonisididae*

Haplotype 25, represented by a single individual, was identified morphologically as *Chelidonis aurantiaca* Studer, 1890. Initially, it was thought to be a keratoisidid due the presence of nodes on the axis, yet no PCR reaction amplified across the characteristic keratoisidid *CO3—mtMutS* gene boundary and instead successfully amplified across the *ND4L—mtMutS* boundary, suggesting it was a different family of bamboo coral. The gross colony morphology of a planar colony with dichotomous branching, and orange coenenchyme (M44, Figure 4c) with six-radiate sclerites (Figure S49), was used to diagnose the species [70]. While six-radiate sclerites are also found in other genera of octocorals such as *Corallium* and *Paragorgia*, this feature in corals with nodes is unique to *Chelidonis*.

3.5. *Uncertainty in Species Estimates*

In total, we believe that there are between 25 and 40 species of octocorals in our dataset (Table 4). The largest uncertainty in estimating the upper and lower bounds in our species estimate is due primarily to the poorly understood species boundaries in Keratoisididae.

We placed the lower bound of our keratoisidid species estimate at 14, the number of potential species delimited by bGMYC when a $p > 0.9$ threshold is applied. Other delimitation methods returned lower species estimates. For example, MT-mPTP inferred corals from multiple subclades comprised a single species. Such scenarios are unrealistic since the Watling et al. subclades contain multiple undescribed genera, thus the lower estimates returned by some delimitation methods were discarded. The upper bound of our keratoisidid species estimate was 27, which was estimated by considering each morphotype (apart from the three morphotypes diagnosed as *A. arbuscula*) as a unique species.

The number of putative species in Primnoidae is six or seven. Five haplotypes were diagnosed to an accepted species rank, which is congruent with the delimitation by bGMYC, ST-GMYC and MT-GMYC. Neither ST-mPTP nor MT-mPTP could successfully delimit these species, and thus we discarded the lower species estimates inferred by those methods. The uncertainty in the absolute number of primnoid species is that the four haplotypes diagnosed as *Primnoa* sp. may represent one species with high haplotypic diversity, or two species as per bGMYC.

There are either four or five species of Chrysogorgiidae in our dataset. Each of Untiedt et al.'s [18] Chrysogorgia groups represents a candidate genera, meaning that there is a minimum of four species present in our data (and potentially five, as there are two haplotypes diagnosed as members of Chrysogorgia Group 7).

There is only one species of Chelidonisididae, *C. aurantiaca*.

4. Discussion

4.1. *Morphological and Genetic Diversity of Calcaxonians*

The morphological diversity of keratoisidids is not reflected in the genetic diversity using a concatenated alignment of *mtMutS*, *COI + igr1*, *16S rRNA-ND2*, and *igr4*. Of the 30 morphotypes observed across the 23 keratoisidid haplotypes recovered, 16 are found within seven haplotypes (Haplotypes 1, 6, 8, 13, 16, 19, and 21). Morphotypes are also shared between haplotypes; for example, M17 is shared between Haplotypes 13 and 14 and M10 between Haplotypes 4 and 6, suggesting that some species may have more genetic diversity in the selected markers than others. The octocoral genus *Paramuricea* was thought to harbour multiple distinct species off Canada due to the high haplotypic diversity present [78]; however, more recent examination of those same individuals using genetic

variation present in single nucleotide polymorphisms (SNPs) generated via Restriction-site Associated DNA sequencing (RADseq) found that there is evidence for a single species with multiple *mtMutS* haplotypes [79]. Multiple putative species have also been observed to share an identical *mtMutS* haplotype: for example, three putative species within the genus *Chrysogorgia* shared a *mtMutS* haplotype [24], and two *Narella* species, *N. hawaiiensis* Cairns and Bayer, 2008 and *N. dichotoma* (Versluys, 1906) shared a single *mtMutS* haplotype [37]. Further genetic work with more variable markers on a wide range of specimens will help untangle what is intraspecific variation and where the species boundaries are.

From our data, there is no consistency in the potential species assignments among genetic delimitation methods, and without additional genome-wide data, it is impossible to accurately define species boundaries. However, it is unlikely that every haplotype or every morphotype represents a distinct species. For example, Haplotype 21 contains three distinct morphotypes (M24, M25, and M26) all diagnosed as *Acanella arbuscula*. *Acanella arbuscula* is known to exhibit a wide range of gross colony morphologies [69], and in this current study, three morphotypes were identified that broadly corresponded to a depth cline. The gross morphology of *A. arbuscula* changed from a loose bush (M24) at ~2000 m to a tight bush (M25) at ~1600 m and finally to a more funnel-shaped bushy colony (M24) at ~1300 m. Phenotypic plasticity along a depth cline has been observed in shallow and mesophotic corals; *Eunicea flexuosa* (Lamouroux, 1821) has a shallow (<5 m) and deep (>17 m) morphotype in the Caribbean [80] and *Briareum asbestinum* (Pallas, 1766) has distinct morphs found at 5 m and 35 m [81].

In Clade I1, Haplotype 13 comprises three morphotypes (M16, M17, and M18) that are vastly different in gross colony morphology and are likely to represent different species rather than phenotypic plasticity. Haplotype 4 and some individuals of Haplotype 6 were diagnosed as being the same morphotype, M10, based on gross morphology. However, they differ in their sclerite composition, with Haplotype 4 having wider flat rods in the tentacles, whereas M10 individuals from Haplotype 6 had narrow elongated rods. Finally, Haplotypes 33, 34, 35, and 36 are all diagnosed as *Primnoa* sp. And all share the same gross colony morphology, M31, which suggests they are all the same species and that there is just high haplotypic diversity within this species using the selected genetic markers. Genetically, the *mtMutS* sequence of Haplotype 34 is identical to *Primnoa notialis* Cairns and Bayer, 2005 (GenBank Accession Number MG986917.1 [20]), *Primnoa pacifica* Kinoshita, 1907 (GenBank Accession number MF319956.1 [82]), and *P. resedaeformis* (GenBank Accession Number MG986945.1 [20]), while Haplotypes 35, 36, and 37 have a single mutation that differentiates them from these sequences (99.87% similarity). This highlights the need for better markers to delimit between species in this genus.

We found using the superextended barcode comprising the four gene regions, chosen based on previous delimitation potential across different families within the suborder Calcaxonia but not previously used as a single multilocus barcode, delimited more haplotypes than any single gene barcode. The species delimiting power of the intergenic spacer between *COB* and *ND6* (*igr4*) within Keratoisididae suggested by van der Ham et al. [36] was further evidenced by our data where 16 *igr4* haplotypes were recovered versus 13 *mtMutS* haplotypes (Table S3). This delimiting power was neither observed in Primnoidae, where the well-established primnoid genera *Narella*, *Candidella*, and *Primnoa* shared a single *igr4* haplotype, nor in Chrysogorgiidae, where *igr4* could not even successfully delimit among all groups of *Chrysogorgia* (*Chrysogorgia* Group 3 and *Dasygorgia* share an *igr4* haplotype; Table S3). When the morphological and molecular species designations of *Narella* were compared, the inclusion of *ND2* with the extended octocoral barcode successfully delimited more species than *mtMutS* and *COI* + *igr1* on its own [37]. The primers for *ND2* capture 209 bp of 16S rRNA, and we included these bases in our alignment because of the increased variation it provided when used with *ND2*. The 16S rRNA-*ND2* genetic fragment yielded 15 keratoisidid haplotypes demonstrating delimiting power in Keratoisididae.

4.2. The Usefulness of Genetic Species Delimitation in Octocorals

The number of potential species genetically delimited varied between 5 and 27 depending on the method of delimitation used. MT-mPTP delimited the fewest species and bGMYC recovered the most (the different species recovered using different p thresholds in bGMYC can be found in Figure S50). Due to the lack of variation in octocoral mitochondrial genes, individuals of different species might have identical DNA sequences at these markers, making it likely that multiple species are represented by a single terminus. Since multiple species potentially share a terminus, genetic species delimitation methods could never delimit the species successfully, and additional avenues of investigation such as morphology are required. The added variability associated with using additional nuclear markers such as 28S may help increase the delimiting power of our concatenated alignment, as seen in the well-studied shallow-water genera *Sinularia* [34,83] and *Ovubunda* [84], and should be included in future barcoding studies. However, some nuclear markers such as the multicopy internal transcribed spacers (ITS1 and ITS2) may not have a shared evolution due to the heterogeneity in copies of ITS in the genome between species [85], limiting their potential usefulness as barcodes.

Where multiple species are represented by a single terminus, the calibration of intraspecific versus interspecific branching rates in GMYC delimitation methods may be affected [86]. The low nucleotide substitution rates within octocoral mitogenomes further limit the effectiveness of substitution-based delimitation methods such as mPTP, as potentially observed where MT-mPTP united all members of Primnoidae as one species and all members of Chrysogorgiidae as another.

bGMYC is believed to have performed the best, as the differences in morphology between individuals both within and between keratoisidid haplotypes suggest that there are more putative species in our samples than recovered by any genetic delimitation, and bGMYC recovered the most species. However, it is accepted that our current knowledge of intraspecific variation in octocorals is limited, and that some species, such as *A. arbuscula*, exhibit a wide range of distinctive morphologies, which must be considered as potential intraspecific variation, when we interpret the number of species present. bGMYC successfully delimited all accepted species in the Primnoidae, delimited species among the different groups within the Chrysogorgiidae, and found that the two morphotypes within *Chrysogorgia s.l.* Group 7 were different species.

4.3. Comparisons of Keratoisidid Diversity with Other Regions

Due to its distinctive gross colony morphology and colouration, *Acanella* is the most easily identifiable bamboo coral for many deep-sea researchers; therefore, there are relatively more records in the literature of individuals within this genus. Along the Irish Margin, coral gardens dominated by *Acanella* species have been reported from the Whittard Canyon at unspecified depths between 520 and 4073 m [23,87], along the Hebrides Slope at 1295 m [88], and the Northern Feni Ridge along the Eastern Rockall Bank at 1920 m [89], with occurrences of the species also reported from the rocky outcrop along the Western Hatton Bank between 1100–1600 m [90] and as bycatch from longlining in this region [91] between 950–2200 m.

Because of taxonomic difficulties in Keratoisididae, specific records of the bamboo species encountered in this study are difficult to source. Dense patches of bamboo corals from subclade D2 have been identified at ~900 m in Baffin Bay between Greenland and Canada [92]. These D2 corals were found anchored into soft sediment and had overall bramble-shaped colonies, which were morphologically distinct from any morphotypes we identified off Ireland. One species of keratoisidid, “Keratoisidinae sp. 1” [93], was found at 1288 m on the Galicia Bank and shared the same polyp morphology as M22 (Figure S24) in subclade J3, suggesting it may represent the same species. Four other keratoisidid species, excluding the previously mentioned *A. arbuscula*, were also collected from the Galicia Bank [93], but none appeared comparable to morphotypes described herein. In comparison with the 14–27 potential species of keratoisidid found in this study,

nine keratoisidid morphotypes were found across 17 peaks of the New England and Corner Rise seamounts, including two that could be diagnosed as *Keratoisidid grayi* Wright, 1869 (D2) and *A. arbuscula* (A1), one morphotype each that was representative of C1, D2, and J3, two morphotypes from subclade D1, and two undescribed species that could not be assigned to a subclade [94]. Our results suggest that the Irish Continental Slope may be an important biodiversity hotspot of keratoisidids; however, further specimens will need to be examined to confirm this.

4.4. Interesting New Occurrence Records

This is the first report of *C. clinata* in Irish waters, and only the second for the Northeast Atlantic, the other being from the Galicia Bank [93]. This species is known from the Northwest Atlantic [64], including the New England and Corner Rise Seamounts [95] (which suggests an Amphi-Atlantic distribution), and from deep waters around New Zealand [96]. Cairns [96] reports that the *C. clinata* specimens from New Zealand are morphologically identical to those reported from the Northwestern Atlantic, where the species was first described by Cairns [64]. Other scleractinian coral species have been found to have the same disjunct distribution: the cup corals *Vaughanella concinna* Gravier, 1915 and *Dasmosmilia lymani* (Pourtales, 1871) are both found in the North Atlantic, The West Pacific, and the deep waters around New Zealand [96].

This is the second record of *C. aurantiaca* from Irish waters, the other being in 1907 [97]. Previously, this species has been identified from Morocco to SW Ireland in the Northeast Atlantic, the Florida Keys to the Bahamas in the Northwest Atlantic, and the Ligurian Sea in the Mediterranean (summarised in [98]). Our record is also the deepest this species has ever been observed at 1507 m (previously 1332 m).

5. Conclusions

While we did not report on an absolute number of species present in our dataset, this study represents a significant improvement in our understanding of the distribution, morphological diversity, and genetic diversity of calcareous octocorals along the Irish continental slope and is the first step towards quantifying the observed biodiversity in the region. Using a superextended barcode (comprising *mtMutS*, *CO1* + *igr1*, 16S rRNA-*ND2*, and *igr4*) and subsequent genetic species delimitation in tandem with a detailed morphological investigation, we estimate that there are between 25 and 40 species of octocorals in our dataset. However, it is clear that further taxonomic work is needed before a more accurate species estimate is possible for the keratoisidids and chrysogorgiids.

Supplementary Materials: The following supporting information can be downloaded at: <https://www.mdpi.com/article/10.3390/d14070576/s1>, Figures S1–S49: Taxonomic plates for every morphotype within every haplotype; Figure S50: bGMYC heatmap; Table S1: Sampling information of all octocorals used in this study; Table S2: Partition information used in the construction of the phylogenetic tree; Table S3: Haplotype breakdown for every individual in this study from every genetic marker used.

Author Contributions: Conceptualization, D.M. and A.L.A.; methodology, D.M., A.L.A., C.B.U., K.C., A.R. and E.T.; formal analysis, D.M. and A.L.A.; writing—original draft preparation, D.M. and A.L.A.; writing—review and editing, D.M., A.L.A. and C.B.U.; supervision, A.L.A. All authors have read and agreed to the published version of the manuscript.

Funding: D. Morrissey is funded by an Irish Research Council Postgraduate Scholarship (GOIPG/2019/3682). The APCs for this publication were funded with the support of the Marine Institute under the Marine Research Programme with the support of the Irish Government. Expeditions (CE17008 and CE18012) of *RV Celtic Explorer* funded by Science Foundation Ireland and the Marine Institute under Investigators Programme Grant SFI/15/IA/3100 and co-funded under the European Regional Development Fund 2014–2020 awarded to A. L. Allcock.

Institutional Review Board Statement: Not applicable.

Data Availability Statement: The sequences and meta data of the specimens were deposited in GenBank. Accession numbers listed in Table 2.

Acknowledgments: Images taken with *ROV Holland I* deployed from *RV Celtic Explorer* copyright Marine Institute. We thank the crew and scientists of cruises CE17008 and CE18012 aboard *RV Celtic Explorer* and the crew operating *ROV Holland I* for all their help. We thank Emma McDermott at the Centre for Microscopy and Imaging, Anatomy, School of Medicine, National University of Ireland Galway for all the Scanning Electron Microscopy images of the sclerites and for advice on sample preparation. D. Morrissey would like to thank Alexa Parimbelli for informative conversations on identifying corals from imagery, and Jamie Maxwell for his GIS skills and critical review of the manuscript. We thank Les Watling for his advice regarding bamboo coral taxonomy and in situ sclerite visualization techniques. Finally, we would like to thank the reviewers for their suggestions and comments which substantially improved the manuscript.

Conflicts of Interest: The authors declare no conflict of interest. The funders had no role in the design of the study; in the collection, analyses, or interpretation of data; in the writing of the manuscript, or in the decision to publish the results.

References

- Ramirez-Llodra, E.; Tyler, P.A.; Baker, M.C.; Bergstad, O.A.; Clark, M.R.; Escobar, E.; Levin, L.A.; Menot, L.; Rowden, A.A.; Smith, C.R.; et al. Man and the last great wilderness: Human impact on the deep sea. *PLoS ONE* **2011**, *6*, e22588. [CrossRef]
- Fernandez-Arcaya, U.; Ramirez-Llodra, E.; Aguzzi, J.; Allcock, A.L.; Davies, J.S.; Dissanayake, A.; Harris, P.; Howell, K.; Huvenne, V.A.I.; Macmillan-Lawler, M.; et al. Ecological Role of Submarine Canyons and Need for Canyon Conservation: A Review. *Front. Mar. Sci.* **2017**, *4*, 5. [CrossRef]
- Morato, T.; Hoyle, S.D.; Allain, V.; Nicol, S.J. Seamounts are hotspots of pelagic biodiversity in the open ocean. *Proc. Natl. Acad. Sci. USA* **2010**, *107*, 9707–9711. [CrossRef]
- Roberts, J.M.; Wheeler, A.J.; Freiwald, A. Reefs of the deep: The biology and geology of cold-water coral ecosystems. *Science* **2006**, *312*, 543–547. [CrossRef]
- Levin, L.A.; Sibuet, M. Understanding continental margin biodiversity: A new imperative. *Ann. Rev. Mar. Sci.* **2012**, *4*, 79–112. [CrossRef]
- White, M.; Dorschel, B. The importance of the permanent thermocline to the cold water coral carbonate mound distribution in the NE Atlantic. *Earth Planet. Sci. Lett.* **2010**, *296*, 395–402. [CrossRef]
- Johnson, M.P.; White, M.; Wilson, A.; Würzberg, L.; Schwabe, E.; Folch, H.; Allcock, A.L. A vertical wall dominated by *Acesta excavata* and *Neopycnodonte zibrowii*, part of an undersampled group of deep-sea habitats. *PLoS ONE* **2013**, *8*, e79917. [CrossRef]
- Pearman, T.R.R.; Robert, K.; Callaway, A.; Hall, R.; Lo Iacono, C.; Huvenne, V.A.I. Improving the predictive capability of benthic species distribution models by incorporating oceanographic data—Towards holistic ecological modelling of a submarine canyon. *Prog. Oceanogr.* **2020**, *184*, 102338. [CrossRef]
- Watling, L.; France, S.C.; Pante, E.; Simpson, A. Biology of Deep-Water Octocorals. In *Advances in Marine Biology*; Lesser, M.B.T.-A., In, M.B., Eds.; Academic Press: Cambridge, MA, USA, 2011; Volume 60, pp. 41–122. ISBN 0065-2881.
- Etnoyer, P.; Warrenchuk, J. A catshark nursery in a deep gorgonian field in the Mississippi Canyon, Gulf of Mexico. *Bull. Mar. Sci.* **2007**, *81*, 553–559.
- Shea, E.K.; Ziegler, A.; Faber, C.; Shank, T.M. Dumbo octopod hatchling provides insight into early cirrate life cycle. *Curr. Biol.* **2018**, *28*, R144–R145. [CrossRef]
- de Neves, B.M.; Wareham Hayes, V.; Herder, E.; Hedges, K.; Grant, C.; Archambault, P. Cold-Water Soft Corals (Cnidaria: Nephtheidae) as Habitat for Juvenile Basket Stars (Echinodermata: Gorgonocephalidae). *Front. Mar. Sci.* **2020**, *7*, 547896. [CrossRef]
- Prouty, N.G.; Fisher, C.R.; Demopoulos, A.W.J.; Druffel, E.R.M. Growth rates and ages of deep-sea corals impacted by the Deepwater Horizon oil spill. *Deep. Res. Part II Top. Stud. Oceanogr.* **2016**, *129*, 196–212. [CrossRef]
- France, S.C. Genetic analysis of bamboo corals (Cnidaria: Octocorallia: Isididae): Does lack of colony branching distinguish *Lepidisis* from *Keratoisis*? *Bull. Mar. Sci.* **2007**, *81*, 323–333.
- Dueñas, L.F.; Alderslade, P.; Sánchez, J.A. Molecular systematics of the deep-sea bamboo corals (Octocorallia: Isididae: Keratoisidinae) from New Zealand with descriptions of two new species of *Keratoisis*. *Mol. Phylogenet. Evol.* **2014**, *74*, 15–28. [CrossRef]
- Watling, L.; Heestand Saucier, E.; France, S.C. Towards a revision of the bamboo corals (Octocorallia): Part 4, delineating the family Keratoisididae. *Zootaxa* **2022**, *5093*, 337–375. [CrossRef]
- Cordeiro, R.; McFadden, C.S.; Van Ofwegen, L.; Williams, G. World List of Octocorallia. Available online: <https://www.marinespecies.org/aphia.php?p=taxdetails&id=125294> (accessed on 25 May 2022).
- Untiedt, C.B.; Quattrini, A.M.; McFadden, C.S.; Alderslade, P.A.; Pante, E.; BurrIDGE, C.P. Phylogenetic Relationships Within Chrysogorgia (Alcyonacea: Octocorallia), a Morphologically Diverse Genus of Octocoral, Revealed Using a Target Enrichment Approach. *Front. Mar. Sci.* **2021**, *7*, 599984. [CrossRef]

19. Taylor, M.L.; Rogers, A.D. Primnoidae (Cnidaria: Octocorallia) of the SW Indian Ocean: New species, genus revisions and systematics. *Zool. J. Linn. Soc.* **2017**, *181*, 70–97. [[CrossRef](#)]
20. Cairns, S.D.; Wirshing, H.H. A phylogenetic analysis of the Primnoidae (Anthozoa: Octocorallia: Calcaxonia) with analyses of character evolution and a key to the genera and subgenera. *BMC Evol. Biol.* **2018**, *18*, 66. [[CrossRef](#)]
21. Núñez-Flores, M.; Gomez-Uchida, D.; López-González, P.J. Molecular systematics of Thouarella (Octocorallia: Primnoidae) with the description of three new species from the Southern Ocean based on combined molecular and morphological evidence. *Invertebr. Syst.* **2021**, *35*, 655–674. [[CrossRef](#)]
22. Davies, J.S.; Stewart, H.A.; Narayanaswamy, B.E.; Jacobs, C.; Spicer, J.; Golding, N.; Howell, K.L. Benthic assemblages of the Anton Dohrn Seamount (NE Atlantic): Defining deep-sea biotopes to support habitat mapping and management efforts with a focus on vulnerable marine ecosystems. *PLoS ONE* **2015**, *10*, e124815. [[CrossRef](#)]
23. Robert, K.; Jones, D.O.B.; Tyler, P.A.; Van Rooij, D.; Huvenne, V.A.I. Finding the hotspots within a biodiversity hotspot: Fine-scale biological predictions within a submarine canyon using high-resolution acoustic mapping techniques. *Mar. Ecol.* **2015**, *36*, 1256–1276. [[CrossRef](#)]
24. Pante, E.; Abdelkrim, J.; Viricel, A.; Gey, D.; France, S.C.; Boisselier, M.C.; Samadi, S. Use of RAD sequencing for delimiting species. *Heredity* **2015**, *114*, 450–459. [[CrossRef](#)] [[PubMed](#)]
25. Herrera, S.; Shank, T.M. RAD sequencing enables unprecedented phylogenetic resolution and objective species delimitation in recalcitrant divergent taxa. *Mol. Phylogenet. Evol.* **2016**, *100*, 70–79. [[CrossRef](#)] [[PubMed](#)]
26. Erickson, K.L.; Pentico, A.; Quattrini, A.M.; McFadden, C.S. New approaches to species delimitation and population structure of anthozoans: Two case studies of octocorals using ultraconserved elements and exons. *Mol. Ecol. Resour.* **2021**, *21*, 78–92. [[CrossRef](#)] [[PubMed](#)]
27. Quattrini, A.M.; Wu, T.; Soong, K.; Jeng, M.S.; Benayahu, Y.; McFadden, C.S. A next generation approach to species delimitation reveals the role of hybridization in a cryptic species complex of corals. *BMC Evol. Biol.* **2019**, *19*, 116. [[CrossRef](#)] [[PubMed](#)]
28. Brasier, M.J.; Wiklund, H.; Neal, L.; Jeffreys, R.; Linse, K.; Ruhl, H.; Glover, A.G. DNA barcoding uncovers cryptic diversity in 50% of deep-sea antarctic polychaetes. *R. Soc. Open Sci.* **2016**, *3*, 160432. [[CrossRef](#)] [[PubMed](#)]
29. Puckridge, M.; Andreakis, N.; Appleyard, S.A.; Ward, R.D. Cryptic diversity in flathead fishes (Scorpaeniformes: Platycephalidae) across the Indo-West Pacific uncovered by DNA barcoding. *Mol. Ecol. Resour.* **2013**, *13*, 32–42. [[CrossRef](#)] [[PubMed](#)]
30. Muthye, V.; Mackereth, C.D.; Stewart, J.B.; Lavrov, D.V. Large dataset of octocoral mitochondrial genomes provides new insights into mt-mutS evolution and function. *DNA Repair* **2022**, *110*, 103273. [[CrossRef](#)]
31. Bilewitch, J.P.; Degnan, S.M. A unique horizontal gene transfer event has provided the octocoral mitochondrial genome with an active mismatch repair gene that has potential for an unusual self-contained function. *BMC Evol. Biol.* **2011**, *11*, 228. [[CrossRef](#)]
32. France, S.C.; Hoover, L.L. DNA sequences of the mitochondrial COI gene have low levels of divergence among deep-sea octocorals (Cnidaria: Anthozoa). *Hydrobiologia* **2002**, *471*, 149–155. [[CrossRef](#)]
33. France, S.C.; Hoover, L.L. Analysis of variation in mitochondrial DNA sequences (ND3, ND4L, MSH) among Octocorallia (=Alcyonaria) (Cnidaria: Anthozoa). *Bull. Biol. Soc. Washingt.* **2001**, *10*, 110–118.
34. McFadden, C.S.; Benayahu, Y.; Pante, E.; Thoma, J.N.; Nevarez, P.A.; France, S.C. Limitations of mitochondrial gene barcoding in Octocorallia. *Mol. Ecol. Resour.* **2011**, *11*, 19–31. [[CrossRef](#)] [[PubMed](#)]
35. Benayahu, Y.; van Ofwegen, L.P.; Dai, C.F.; Jeng, M.S.; Soong, K.; Shlagman, A.; Du, S.W.; Hong, P.; Imam, N.H.; Chung, A.; et al. The octocorals of dongsha atoll (South China sea): An iterative approach to species identification using classical taxonomy and molecular barcodes. *Zool. Stud.* **2018**, *57*, e50. [[CrossRef](#)]
36. van der Ham, J.L.; Brugler, M.R.; France, S.C. Exploring the utility of an indel-rich, mitochondrial intergenic region as a molecular barcode for bamboo corals (Octocorallia: Isididae). *Mar. Genomics* **2009**, *2*, 183–192. [[CrossRef](#)]
37. Baco, A.R.; Cairns, S.D. Comparing molecular variation to morphological species designations in the deep-sea coral *Narella* reveals new insights into seamount coral ranges. *PLoS ONE* **2012**, *7*, e45555. [[CrossRef](#)]
38. Ross, L.K.; Ross, R.E.; Stewart, H.A.; Howell, K.L. The influence of data resolution on predicted distribution and estimates of extent of current protection of three “listed” deep-sea habitats. *PLoS ONE* **2015**, *10*, e140061. [[CrossRef](#)]
39. Esri Inc. *ArcGIS Pro*; Version 2.8; Esri Inc.: Redlands, CA, USA, 2020.
40. Kearse, M.; Moir, R.; Wilson, A.; Stones-Havas, S.; Cheung, M.; Sturrock, S.; Buxton, S.; Cooper, A.; Markowitz, S.; Duran, C.; et al. Geneious Basic: An integrated and extendable desktop software platform for the organization and analysis of sequence data. *Bioinformatics* **2012**, *28*, 1647–1649. [[CrossRef](#)]
41. Edgar, R.C. MUSCLE: Multiple sequence alignment with high accuracy and high throughput. *Nucleic Acids Res.* **2004**, *32*, 1792–1797. [[CrossRef](#)]
42. Kumar, S.; Stecher, G.; Li, M.; Nnyaz, C.; Tamura, K. MEGA X: Molecular evolutionary genetics analysis across computing platforms. *Mol. Biol. Evol.* **2018**, *35*, 1547–1549. [[CrossRef](#)]
43. Katoh, K.; Standley, D.M. MAFFT multiple sequence alignment software version 7: Improvements in performance and usability. *Mol. Biol. Evol.* **2013**, *30*, 772–780. [[CrossRef](#)]
44. Brugler, M.R.; France, S.C. The mitochondrial genome of a deep-sea bamboo coral (Cnidaria, Anthozoa, Octocorallia, Isididae): Genome structure and putative origins of replication are not conserved among octocorals. *J. Mol. Evol.* **2008**, *67*, 125. [[CrossRef](#)] [[PubMed](#)]

45. Sanchez, J.A.; McFadden, C.; France, S.; Lasker, H. Molecular Phylogenetic analyses of shallow-water Caribbean octocorals. *Mar. Biol.* **2003**, *142*, 975–987. [[CrossRef](#)]
46. Pante, E.; France, S.C.; Couloux, A.; Cruaud, C.; McFadden, C.S.; Samadi, S.; Watling, L. Deep-sea origin and in-situ diversification of chrysogorgiid octocorals. *PLoS ONE* **2012**, *7*, e38357. [[CrossRef](#)] [[PubMed](#)]
47. McFadden, C.S.; Tullis, I.D.; Breton Hutchinson, M.; Winner, K.; Sohm, J.A. Variation in Coding (NADH Dehydrogenase Subunits 2, 3, and 6) and Noncoding Intergenic Spacer Regions of the Mitochondrial Genome in Octocorallia (Cnidaria: Anthozoa). *Mar. Biotechnol.* **2004**, *6*, 516–526. [[CrossRef](#)] [[PubMed](#)]
48. Easton, E.E.; Hicks, D. 161 Primers for PCR-Amplification of Octocorallia Mitochondrial Genome Fragments. Available online: https://figshare.com/articles/dataset/161_primers_for_PCR-amplification_of_Octocorallia_mitochondrial_genome_fragments/19617519 (accessed on 3 May 2022).
49. Clement, M.; Posada, D.; Crandall, K.A. TCS: A computer program to estimate gene genealogies. *Mol. Ecol.* **2000**, *9*, 1657–1659. [[CrossRef](#)]
50. Templeton, A.R.; Crandall, K.A.; Sing, C.F. A cladistic analysis of phenotypic associations with haplotypes inferred from restriction endonuclease mapping and DNA sequence data. III. Cladogram estimation. *Genetics* **1992**, *132*, 619–633. [[CrossRef](#)]
51. Nguyen, L.T.; Schmidt, H.A.; Von Haeseler, A.; Minh, B.Q. IQ-TREE: A fast and effective stochastic algorithm for estimating maximum-likelihood phylogenies. *Mol. Biol. Evol.* **2015**, *32*, 268–274. [[CrossRef](#)]
52. Lanfear, R.; Calcott, B.; Ho, S.Y.W.; Guindon, S. PartitionFinder: Combined selection of partitioning schemes and substitution models for phylogenetic analyses. *Mol. Biol. Evol.* **2012**, *29*, 1695–1701. [[CrossRef](#)]
53. Felsenstein, J. Confidence Limits on Phylogenies: An Approach Using the Bootstrap. *Evolution* **1985**, *39*, 783. [[CrossRef](#)]
54. Saucier, E.H.; France, S.C.; Watling, L. Toward a revision of the bamboo corals: Part 3, deconstructing the Family Isididae. *Zootaxa* **2021**, *5047*, 247–272. [[CrossRef](#)]
55. Hebert, P.D.N.; Ratnasingham, S.; DeWaard, J.R. Barcoding animal life: Cytochrome c oxidase subunit 1 divergences among closely related species. *Proc. R. Soc. B Biol. Sci.* **2003**, *270*, S96–S99. [[CrossRef](#)] [[PubMed](#)]
56. Pons, J.; Barraclough, T.G.; Gomez-Zurita, J.; Cardoso, A.; Duran, D.P.; Hazell, S.; Kamoun, S.; Sumlin, W.D.; Vogler, A.P. Sequence-based species delimitation for the DNA taxonomy of undescribed insects. *Syst. Biol.* **2006**, *55*, 595–609. [[CrossRef](#)]
57. Reid, N.M.; Carstens, B.C. Phylogenetic estimation error can decrease the accuracy of species delimitation: A Bayesian implementation of the general mixed Yule-coalescent model. *BMC Evol. Biol.* **2012**, *12*, 196. [[CrossRef](#)]
58. Zhang, J.; Kapli, P.; Pavlidis, P.; Stamatakis, A. A general species delimitation method with applications to phylogenetic placements. *Bioinformatics* **2013**, *29*, 2869–2876. [[CrossRef](#)]
59. Bouckaert, R.; Heled, J.; Kühnert, D.; Vaughan, T.; Wu, C.H.; Xie, D.; Suchard, M.A.; Rambaut, A.; Drummond, A.J. BEAST 2: A Software Platform for Bayesian Evolutionary Analysis. *PLoS Comput. Biol.* **2014**, *10*, e1003537. [[CrossRef](#)]
60. Douglas, J.; Zhang, R.; Bouckaert, R. Adaptive dating and fast proposals: Revisiting the phylogenetic relaxed clock model. *PLoS Comput. Biol.* **2021**, *17*, e1008322. [[CrossRef](#)]
61. Fujisawa, T.; Ezard, T.; Barraclough, T.G. Splits: Species' limits by threshold statistics. *R Packag. Version* **2013**, *1*, r29.
62. Cairns, S.D.; Bayer, F.M. Studies on western Atlantic Octocorallia (Coelenterata: Anthozoa). Part 5: The genera Plumarella Gray, 1870; Acanthoprimnoa, n. gen.; and Candidella Bayer, 1954. *Proc. Biol. Soc. Washingt.* **2004**, *117*, 447–487.
63. Cairns, S.D. Studies on western Atlantic Octocorallia (Coelenterata: Anthozoa). Part 6: The genera Primnoella Gray, 1858; Thouarella Gray, 1870; Dasystemella Versluys, 1906. *Proc. Biol. Soc. Washingt.* **2006**, *119*, 161–194. [[CrossRef](#)]
64. Cairns, S.D. Studies on western Atlantic Octocorallia (Gorgonacea: Primnoidae). Part 8: New records of Primnoidae from the New England and Corner Rise Seamounts. *Proc. Biol. Soc. Washingt.* **2007**, *120*, 243–263. [[CrossRef](#)]
65. Cairns, S.D.; Bayer, F.M. A review of the genus Primnoa (Octocorallia: Gorgonacea: Primnoidae), with the description of two new species. *Bull. Mar. Sci.* **2005**, *77*, 225–256.
66. Cairns, S.D.; Taylor, M.L. An illustrated key to the species of the genus narella (Cnidaria, octocorallia, primnoidae). *Zookeys* **2019**, *822*, 1–15. [[CrossRef](#)]
67. Taylor, M.L.; Cairns, S.D.; Agnew, D.J.; Rogers, A.D. A revision of the genus Thouarella Gray, 1870 (Octocorallia: Primnoidae), including an illustrated dichotomous key, a new species description, and comments on Plumarella Gray, 1870 and Dasystemella, Versluys, 1906. *Zootaxa* **2013**, *3602*, 1–105. [[CrossRef](#)] [[PubMed](#)]
68. Watling, L.; France, S.C. A new genus and species of bamboo coral (Octocorallia: Isididae: Keratoisidinae) from the New England seamounts. *Bull. Peabody Museum Nat. Hist.* **2011**, *52*, 209–221. [[CrossRef](#)]
69. Saucier, E.H.; Sajjadi, A.; France, S.C. A taxonomic review of the genus Acanella (Cnidaria: Octocorallia: Isididae) in the North Atlantic Ocean, with descriptions of two new species. *Zootaxa* **2017**, *4323*, 359–390. [[CrossRef](#)]
70. Bayer, F.M.; Stefani, J. New and previously known taxa of isidid octocorals (Coelenterata: Gorgonacea), partly from Antarctic waters. *Proc. Biol. Soc. Washingt.* **1987**, *100*, 937–991.
71. Hadley, A. CombineZP—Image Stacking Software. 2010. Available online: <https://combinezp.software.informer.com/> (accessed on 3 May 2022).
72. Bayer, F.M.; Grasshoff, M.; Verseveldt, J. *Illustrated Trilingual Glossary of Morphological and Anatomical Terms Applied to Octocorallia*; Brill Archive: Leiden, The Netherlands, 1983; ISBN 9004071393.
73. Hogan, R.; Hopkins, K.; Wheeler, A.; Allcock, A.; Yesson, C. Novel diversity in mitochondrial genomes of deep-sea Pennatulacea (Cnidaria: Anthozoa: Octocorallia). *Mitochondrial DNA Part A* **2019**, *30*, 764–777. [[CrossRef](#)]

74. Watling, L.; France, S.C. Toward a revision of the bamboo corals: Part 2, untangling the genus *Lepidisis* (Octocorallia: Isididae). *Bull. Peabody Museum Nat. Hist.* **2021**, *62*, 97–110. [[CrossRef](#)]
75. Dueñas, L.; Sanchez, J.A. Character lability in deep-sea bamboo corals (Octocorallia, Isididae, Keratoisidinae). *Mar. Ecol. Prog. Ser.* **2009**, *397*, 11–23. [[CrossRef](#)]
76. Grasshoff, M. Die Gorgonaria des Expeditionen von “Travailleur” 1880–1882 und “Talisman” 1883 (Cnidaria, Anthozoa). *Bull. Du Muséum Natl. D’histoire Nat. Sect. A Zool. Biol. Écologie Anim.* **1986**, *8*, 9–38.
77. Alderslade, P.; McFadden, C.S. A new genus and species of the family Isididae (Coelenterata: Octocorallia) from a CMAR Biodiversity study, and a discussion on the subfamilial placement of some nominal isidid genera. *Zootaxa* **2012**, *3154*, 21–39. [[CrossRef](#)]
78. Radice, V.Z.; Quattrini, A.M.; Wareham, V.E.; Edinger, E.N.; Cordes, E.E. Vertical water mass structure in the North Atlantic influences the bathymetric distribution of species in the deep-sea coral genus *Paramuricea*. *Deep. Res. Part I Oceanogr. Res. Pap.* **2016**, *116*, 253–263. [[CrossRef](#)]
79. Quattrini, A.M.; Herrera, S.; Adams, J.M.; Grinyó, J.; Allcock, A.L.; Shuler, A.; Wirshing, H.H.; Cordes, E.E.; McFadden, C.S. Phylogeography of *Paramuricea*: The Role of Depth and Water Mass in the Evolution and Distribution of Deep-Sea Corals. *Front. Mar. Sci.* **2022**, *9*, 849402. [[CrossRef](#)]
80. Prada, C.; Schizas, N.V.; Yoshioka, P.M. Phenotypic plasticity or speciation? A case from a clonal marine organism. *BMC Evol. Biol.* **2008**, *8*, 47. [[CrossRef](#)]
81. West, J.M.; Harvell, C.D.; Walls, A.M. Morphological plasticity in a gorgonian coral (*Briareum asbestinum*) over a depth cline. *Mar. Ecol. Prog. Ser.* **1993**, *94*, 61–69. [[CrossRef](#)]
82. Everett, M.V.; Park, L.K. Exploring deep-water coral communities using environmental DNA. *Deep. Res. Part II Top. Stud. Oceanogr.* **2018**, *150*, 229–241. [[CrossRef](#)]
83. McFadden, C.S.; Brown, A.S.; Brayton, C.; Hunt, C.B.; van Ofwegen, L.P. Application of DNA barcoding in biodiversity studies of shallow-water octocorals: Molecular proxies agree with morphological estimates of species richness in Palau. *Coral Reefs* **2014**, *33*, 275–286. [[CrossRef](#)]
84. McFadden, C.S.; Haverkort-Yeh, R.; Reynolds, A.M.; Halász, A.; Quattrini, A.M.; Forsman, Z.H.; Benayahu, Y.; Toonen, R.J. Species boundaries in the absence of morphological, ecological or geographical differentiation in the Red Sea octocoral genus *Ovabunda* (Alcyonacea: Xeniidae). *Mol. Phylogenet. Evol.* **2017**, *112*, 174–184. [[CrossRef](#)]
85. Calderón, I.; Garrabou, J.; Aurelle, D. Evaluation of the utility of COI and ITS markers as tools for population genetic studies of temperate gorgonians. *J. Exp. Mar. Biol. Ecol.* **2006**, *336*, 184–197. [[CrossRef](#)]
86. Dellicour, S.; Flot, J.F. The hitchhiker’s guide to single-locus species delimitation. *Mol. Ecol. Resour.* **2018**, *18*, 1234–1246. [[CrossRef](#)]
87. Morris, K.J.; Tyler, P.A.; Masson, D.G.; Huvenne, V.I.A.; Rogers, A.D. Distribution of cold-water corals in the Whittard Canyon, NE Atlantic Ocean. *Deep. Res. Part II Top. Stud. Oceanogr.* **2013**, *92*, 136–144. [[CrossRef](#)]
88. Roberts, J.M.; Harvey, S.M.; Lamont, P.A.; Gage, J.D.; Humphery, J.D. Seabed photography, environmental assessment and evidence for deep-water trawling on the continental margin west of the Hebrides. *Hydrobiologia* **2000**, *441*, 173–183. [[CrossRef](#)]
89. Hughes, D.J.; Gage, J.D. Benthic metazoan biomass, community structure and bioturbation at three contrasting deep-water sites on the northwest European continental margin. *Prog. Oceanogr.* **2004**, *63*, 29–55. [[CrossRef](#)]
90. Sayago-Gil, M.; Durán-Muñoz, P.; Javier Murillo, F.; Díaz-del-Río, V.; Serrano, A.; Miguel Fernández-Salas, L. A study of Geomorphological Features of the Seabed and the Relationship to Deep-Sea Communities on the Western Slope of Hatton Bank (Ne Atlantic Ocean). In *Seafloor Geomorphology as Benthic Habitat*; Harris, P.T., Baker, E.K., Eds.; Elsevier: Amsterdam, The Netherlands, 2012; pp. 751–761. ISBN 9780123851406.
91. Durán Muñoz, P.; Murillo, F.J.; Sayago-Gil, M.; Serrano, A.; Laporta, M.; Otero, I.; Gómez, C. Effects of deep-sea bottom longlining on the Hatton Bank fish communities and benthic ecosystem, north-east Atlantic. *J. Mar. Biol. Assoc. UK* **2011**, *91*, 939–952. [[CrossRef](#)]
92. de Neves, B.M.; Edinger, E.; Hillaire-Marcel, C.; Saucier, E.H.; France, S.C.; Treble, M.A.; Wareham, V.E. Deep-water bamboo coral forests in a muddy Arctic environment. *Mar. Biodivers.* **2015**, *45*, 867–871. [[CrossRef](#)]
93. Altuna, Á.; Ríos, P.; De Gijón, C.O.; De Oceanografía, I.E.; Asturias, C.P. De Calcaxonian octocorals (Cnidaria: Anthozoa) from demersales, ecomarg and indemares expeditions to bathyal waters off north and northwest Spain (northeast Atlantic). In *Proceedings of the XVIII Iberian Symposium of Marine Biology Studies, Donostia-San Sebastián, Spain, 11–14 September 2012*; p. 33212.
94. Lapointe, A.; Watling, L.; Gontz, A.M. Deep-sea benthic megafaunal communities on the New England and Corner Rise Seamounts, Northwest Atlantic Ocean. In *Seafloor Geomorphology as Benthic Habitat*; Harris, P.T., Baker, E., Eds.; Elsevier: Amsterdam, The Netherlands, 2020; pp. 917–932. ISBN 978-0-12-814960-7.
95. Lapointe, A.E.; Watling, L.; France, S.C.; Auster, P.J. Megabenthic assemblages in the lower bathyal (700–3000 m) on the New England and Corner Rise Seamounts, Northwest Atlantic. *Deep. Res. Part I Oceanogr. Res. Pap.* **2020**, *165*, 103366. [[CrossRef](#)]
96. Cairns, S.D. The marine fauna of New Zealand: New Zealand primnoidea (anthozoa: Alcyonacea) part 1. genera *narella*, *narelloides*, *metanarella*, *calyptrophora*, and *helicoprimum*. *NIWA Biodivers. Mem.* **2012**, *126*, 5–72.

-
97. Stephens, J. *Alcyonarian and Madreporarian Corals of the Irish Coasts*; HM Stationery Office: London, UK, 1909.
 98. Bo, M.; Coppari, M.; Betti, F.; Massa, F.; Gay, G.; Cattaneo-Vietti, R.; Bavestrello, G. Unveiling the deep biodiversity of the Janua Seamount (Ligurian Sea): First Mediterranean sighting of the rare Atlantic bamboo coral *Chelidonisis aurantiaca* Studer, 1890. *Deep. Res. Part I Oceanogr. Res. Pap.* **2020**, *156*, 103186. [[CrossRef](#)]